Altered Expression of Kinetochore Proteins (CENP-A and Mad2) to Explore Chromosome Instability and Aneuploidy

Biology Honors Thesis

Katherine J. Aney '18

Department of Biology
Gustavus Adolphus College
St. Peter, MN 56082

Honors Thesis Committee
Dr. Laura Burrack, Advisor, Department of Biology
Dr. Tom LoFaro, Department of Mathematics
Dr. Jeff Dahlseid, Department of Biology and Chemistry
Dr. Sanjive Qazi, Department of Biology

Acknowledgments

I would like to express my deepest gratitude to Dr. Laura Burrack for her countless hours of assistance during my time at Gustavus. I am extremely thankful for her thoughtful feedback, guidance and dedication to this project. Her mentorship has inspired me, grown my passion for learning and enhanced my Gustavus experience. I would also like to thank the other members of my thesis committee- Dr. Tom LoFaro, Dr. Jeff Dahlseid and Dr. Sanjive Qazi for their assistance and time. A special thanks to Dr. Jeff Boatman and Dr. Laura Boehm Vock for assisting in the math modeling portion of the project and to Erica Power for assisting with laboratory work. Project funding was provided through a grant from the local Sigma Xi chapter and the Gustavus Biology Department. Finally, I would like to thank Gustavus Adolphus College for providing space, materials and laboratory equipment, as well as for their support for undergraduate research.

Introduction

Cancers vary widely, with over 100 well defined types. The mutational patterns that define cancer type and diagnosis are unique and subtypes within cancers further diversify the disease. For example, breast cancer tumors have three main classes- estrogen receptor alpha (ER) positive, human epidermal growth factor receptor 2 (HER2) positive or triple-negative (which do not have ER, HER2 or progesterone receptor mutations) (Fallah et al., 2017). Within these three categories, other oncogenic mutations can further diversify the tumor type, with mutations in genes such as MYC, p53 or RB commonly found within each breast cancer subtype. Additionally, different mutational patterns can occur within a single tumor and can lead to tumor heterogeneity. Despite the many different cancer types, subtypes and mutations, they all share a common characteristic of genome instability (Hanahan and Weinberg, 2011; Negrini et al., 2010). Genome instability typically arises from mutations that alter genes or from chromosome instability (CIN).

Over time, every cell within the body acquires mutations, but most do not affect an organism's health. Somatic mutations are alterations that occur in the DNA of a cell and are be passed on to the next generation when the cell divides. Occasionally, however, these somatic mutations in cells can led to a cancer phenotype. These mutations are called "drivers" because they give the cell a selective advantage that aid in growth and survival. As mentioned above, cancers are extremely variable in the number of somatic mutations they carry, ranging from 0.001 mutations per megabase to over 400 mutations per megabase (Alexandrov et al., 2013). These somatic mutation types or "signatures" are different for different cancers as well as different within a single cancer type (Lawrence et al., 2013). There are approximately 140 known "driver" genes that can contribute to cancer

Dance of the phosphate backbone

Chromatids connect C to

G- Jumbling jargon joined to

T twinned twists to

A- All-together arranging activity

development when mutated. Typically 2-8 “driver” mutations are needed for cancer to develop (Vogelstein et al., 2013). These driver mutations are often the result of point mutations, or small-scale changes to the DNA that may cause amplifications or deletions of genes.

Another cause of genome instability is chromosome instability (CIN), which results from missegregation that causes chromosome abnormalities, such as amplifications, deletions or aneuploidy (an abnormal number of chromosomes, Figure 1 modified from Holland and Cleveland, 2012). Aneuploidy is seen in more than 90% of solid tumors and in more than 75% of hematopoietic tumors (Weaver and Cleveland, 2006). Data suggests that CIN can contribute to the development of the cancer phenotype. When mice are transformed to have CIN, aneuploidy and tumorigenesis are often observed as a result (Schvartzman et al., 2010). This is also seen in human cell lines, where altering genes to cause chromosome instability is sufficient to cause aneuploidy (Land et al, 1983; Vader and Lens, 2008). Cancers with CIN have been shown to have greater resistance to chemotherapeutic drugs (McClelland et al., 2009; Swanton et al., 2009) and CIN in human tumors can be used as a prognostic predictor for the aggressiveness of the cancer (Sheltzer, 2013; Lagarde et al., 2012, Choi et al. 2009; Heilig et al, 2010).

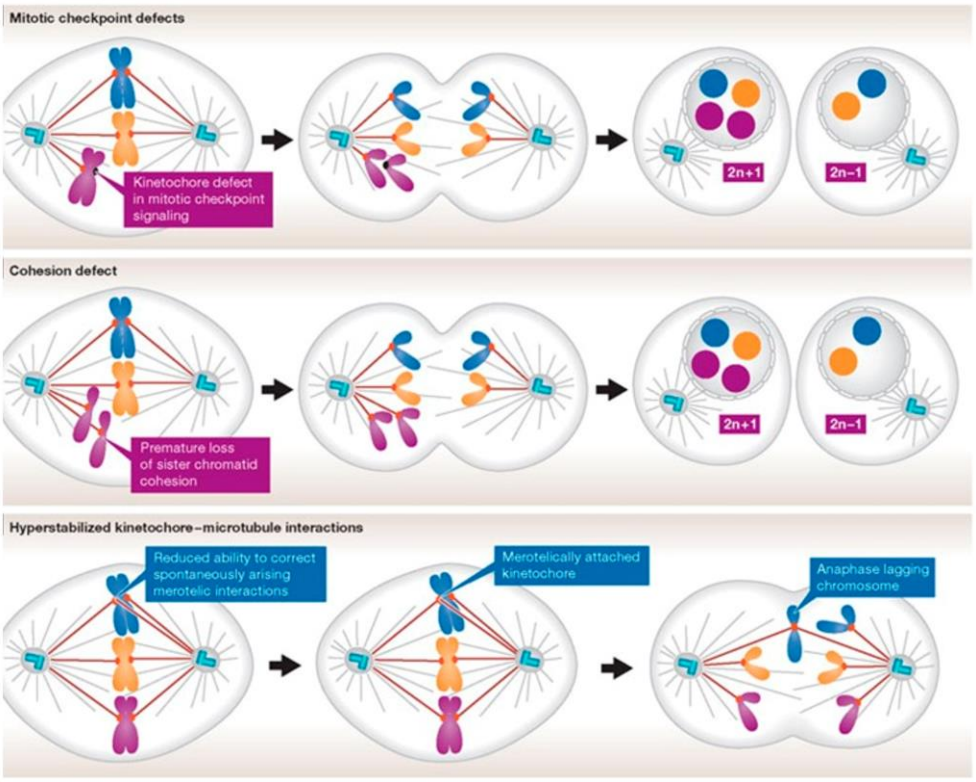

Figure 1: Illustrations of mechanisms that could lead to aneuploidy in cells, including mitotic checkpoint defects, cohesion defects and the opposite problem- hyperstabilized kinetochore-microtubule interactions. The result of each error are shown (figure modified from Holland and Cleveland, 2012).

Mitosis

In dividing cells, DNA that contains the genetic material is split equally into two daughter cells during mitosis. Once DNA is replicated, chromosomes segregation occurs. First, the cell undergoes prophase, where the chromosomes line up in the center of the cell. Next, the cell enters metaphase, where microtubules from spindle pole bodies on opposites sides of the cell attach to the kinetochore protein complex at a region of the chromosome called the centromere. Finally, the two arms of the chromosomes are pulled apart during anaphase and the cell completes division by splitting into two daughter cells during telophase. A cancer phenotype can occur when genes involved in cell division or mitosis are altered (in their expression or function) through mutations or chromosome instability.

spindle assembly checkpoint (SAC)

We connect. To disconnect. To reconnect again. The connections keep us human, grounded. They give us the pieces we are missing. Patience, bravery, inspiration, decisiveness. The connections are vital for life, growth, and repair. We reach with fibers, polymerizing methodically in hopes of finding a place to anchor ourselves. Some attachments are stable. Others are not. The hearts we attach to are more complex than they seem. Hundreds of parts in beautiful coordination and harmony, and we trust that everything falls into place. Once we hold on, we don't let go. We look for a clue, hint, or sign that attachment is right. We have defense mechanisms in place to protect us from harm

Metaphase. Attachments secure. Double check.

Triple check.

Anaphase.

Cell cycle checkpoints

An important mitosis regulator is the spindle assembly checkpoint (SAC), which ensures chromosomes are securely attached to the microtubules that facilitate chromosome separation. At unattached chromosomes, the mitotic checkpoint complex (MCC) binds to the anaphase-promoting complex (APC/C) to prevent cells from dividing before attachments are made. Once the chromosomes are correctly aligned and spindle fibers are attached to the kinetochore, the MCC is degraded, APC/C is activated, and the cell progresses into anaphase (Figure 2, from Sivakumar and Gorbsky, 2015). The MCC is composed of proteins MAD2, BUBR1, BUB3 and CDC20.

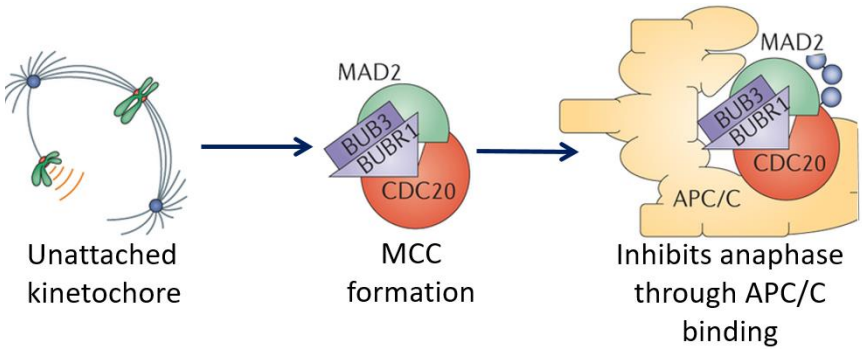

Figure 2: MCC and APC/C binding prevents premature anaphase from occuring (figure modified from Sivakumar and Gorbsky, 2015).

MAD2 dysregulation in cancers

The proteins of the MCC (MAD2, BUB3, BUBR1 and CDC20) have been extensively studied, since unstable kinetochore-microtubule attachments are known to lead to CIN (a hallmark of cancer). Because proteins of the MCC are involved in a critical step that protects against CIN, they are often found dysregulated in cancer. The MCC member, mitotic arrest deficient-like 2 (MAD2) protein has been highly studied and examined in the context of cancers. In human cancers, *MAD2L2* (the gene for MAD2) is seen upregulated in many cancers including large B-cell lymphoma, breast cancer, liver cancer, lung adenocarcinomas, colorectal cancer, soft-tissue sarcomas and gastric cancers (Alizadeh, et al., 2000., Chen et al., 2002, Garber et al., 2001, Hernando et al., 2004, Hisaoka et al., 2008,, Li et al., 2003, Percy et al., 2000, Rimkus et al., 2007, Tanaka et al., 2001, van't Veer et al., 2002, Wang et al., 2009). Further, many studies found *MAD2L2* levels to be an indicator of prognosis, with higher levels associated with poor outcomes (Hisaoka et al., 2008, Li et al., 2003, Percy et al., 2000, Rimkus et al., 2007, Tanaka et al., 2001, van't Veer et al., 2002, Wang et al., 2009). NDC80 is a kinetochore protein that recruits MAD2 to the kinetochore. When NDC80's orthologue, *HEC1*, is overexpressed in transgenic mice, it can initiate tumor formation along with aneuploidy (Diaz-Rodriguez, 2011).

Although overexpression of *MAD2* is seen in many cancer types, there are also cancer types that have *MAD2* under expression. In a study on renal cell carcinoma (RCC), a kidney cancer, papillary RCC had transcriptional overexpression of *MAD2*, while chromophobe RCC had transcriptional under expression of *MAD2* (Pinto et al., 2007). Interestingly, the under expression of *MAD2* has also repeatedly been shown to be related to tumorigenesis. In human cancer

MAD2 -196AA

Mad2'**S** **Q**uaint **S**tory **I**s **S**pent **L**oo**K**in**G** and **STR**iving

To **V**erify **T**h**E** **F**aith**F**ul **E**lderl**Y** Cell's **S**p**IN**dle**S** Are Intactl**LY** Joined,

Qualifying P**R**operly **G**rown & **V**er**Y** **P**rep**A**r**ED** Cells

For **V**i**T**al & **V**aluble Brea**KK**ing

cells and mouse embryonic fibroblasts, deletion of one *MAD2* allele results in higher rates of chromosome missegregation, CIN and aneuploidy (Michel et al., 2001). These mice were shown to express the MAD2 protein at levels that were 70% of control cell expression. Additionally, mice with *MAD2* allele deletions have higher rates of lung tumorigenesis, with 27.5% tumor formation at 18 months of age, compared to no tumors observed in the *MAD2* wild type mice (Michel et al., 2001).

In human cancer cells, under expression of *MAD2* is found in several cell lines including T47D, MDA_MB-361 and BT-549, which all have mitotic checkpoint deficiencies (Percy et al., 2000; Li and Benezra, 1996). In hepatocellular carcinoma (a type of liver cancer), MAD2 protein under expression was significantly associated with cells that had defective mitotic checkpoints (Sze et al., 2004). Another study on nasopharyngeal carcinoma (NPC) showed that cells with low levels of MAD2 protein also had defective mitotic cell cycle checkpoints, as shown through differential mitotic drug responses (Wang et al., 2000). Similar results were seen in ovarian carcinoma (Wang et al., 2002). Further, when the *MAD2* under expressed cells lines were transformed with an inducible system that increased levels of *MAD2*, mitotic checkpoint behavior was restored to normal.

Along with the evidence for dysregulation of *MAD2* in cancer, there is also evidence that dysregulation of *MAD2* with another driver mutation may lead to a cancer phenotype. In mice, *MAD2* overexpression alongside an oncogene activator (*K-Ras*) causes CIN that leads to tumors twice as large as when the oncogene was amplified alone (Figure 3 modified from Sotillo et al., 2010). In these mice, survival was much lower for mice with both *K-ras* or *MAD2* mutations ($p<0.0001$) and tumor relapse was seen in 11 of the 24 mice (compared to no tumor relapse in control mice with *K-ras* mutations only). This suggests that the CIN caused by an oncogene (*K-ras*) alongside *MAD2* deletion may cause aneuploidy. Similarly, *MAD2* and *p53* depleted mice (*MAD2*+/- p53+/-) have significantly increased tumor number and

frequency compared to control mice with *p53* depletion only (*p53+/-)* (Chi et al., 2009). The *MAD2+/- p53+/-* mice also had significantly lower survival rates over time compared to the *p53+/-* mice (p=0.034).

The above cases suggest that MAD2's function relies on a particular level of expression in the cell. This may be related to the importance of the protein's stoichiometry. In humans, MAD2 is found in both open (O-MAD2) and closed (C-MAD2) conformations, which dimerize to each other. This dimerization helps convert the O-MAD2 into C-MAD2 that then binds to CDC20 to form the MCC (Nezi et al., 2006). Only the C-MAD2 can bind to CDC20. Thus, up or down regulation of the protein may affect the stoichiometry and the amount of bound C-MAD2, which could disrupt the spindle assembly checkpoint. This conformational importance could potentially explain how both high and low expression of *MAD2* (relative to normal) are seen in cancers and could explain how altered levels create a stoichiometric imbalance that would be detrimental to the cell.

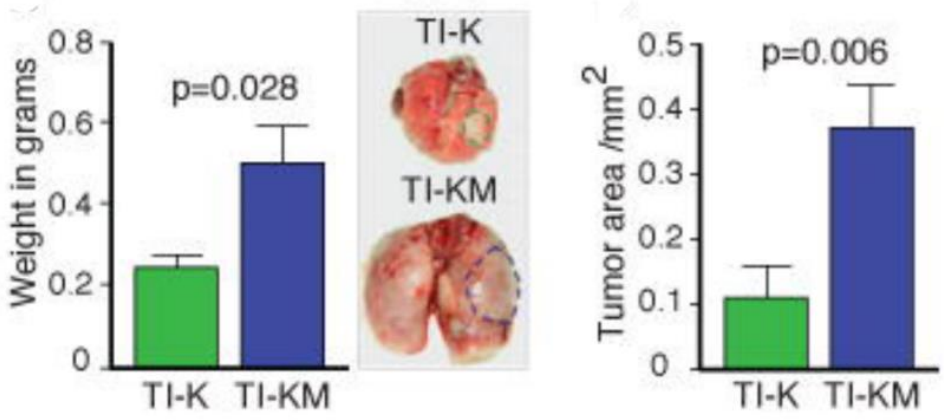

Figure 3: *MAD2* amplification with *K-ras* (TI-KM) leads to significantly larger tumors (both in weight and area) than tumors from the *K-ras* mutation alone (figure modified from Sotillo et al., 2010).

CENP-A overexpression in cancers

Other mitotic processes have been shown to be related to CIN and aneuploidy. The kinetochore is composed of over 50 proteins and the copy number of the kinetochore proteins varies widely among different organisms. CENP-A is a key protein in the kinetochore and is essential for its assembly (Figure 4). Further, complete loss of CENP-A always results in lethality, as it is needed for cells to divide (Verdaasdonk et al., 2011). CENP-A is a histone H3 variant that forms the base of the kinetochore upon which the complex is assemble on.

High expression levels of CENP-A are reported in over 20 solid cancer types (Sun et al., 2016, Lin et al., 2017; Tomonaga et al., 2003) including breast cancer, gastric cancer, colorectal cancer and lung cancer. A comprehensive analysis of 20 CENP-A overexpressing cancers show that elevated expression is correlated with poor prognosis and tumor progression (Sun et al., 2016). In lung adenocarcinoma, high CENP-A expression levels are

CENP-A

Do you ever think of letting go
or how tight you hold on
or what would happen if you slow
your hard work or were gone?

You hold your DNA so close
and every day repeat
the process so that nothing slows
and cells don't miss a beat.

Your neighborhood's been organized
with participation vital
and everything's familiarized,
there's no time for recital.

I know you don't know but it's true, I know it seems like déjà vu
but if you doubt or question things--stability relies on you.

also significantly correlated with shorter survival time and CENP-A can be used as a prognosis factor for diagnosing patients (Wu et al., 2012). Another bioinformatics study identified 14 centromere and kinetochore proteins commonly overexpressed in cancers and half of the identified proteins were involved in CENP-A nucleosome formation (Zhang et al., 2016). Using these genes, a "Centromere and kinetochore gene Expression Score" (CES) was developed and compared to genome instability (measured by copy number alterations and mutational frequency). Significant positive correlation was seen between CES and both copy number alteration and mutational frequency in 7 cancer types (39% of the studied cancers), including breast, lung, stomach and brain gliomas. In the other cancer types analyzed, 33% had one of the two genome instability types (copy number alterations or mutational frequency) positively correlated to CES. The model was also able to predict survival in patients, where patients with a higher CES had significantly worse prognosis (Figure 5, modified from Zhang et al., 2016). This was analyzed for subsets of breast and lung cancers and significance was found in each case (log-rank p-value ranging from 0.024 to 4.9×10^{-9}).

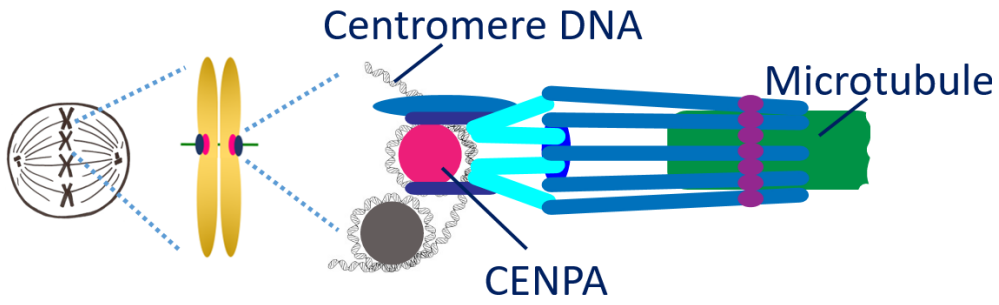

Figure 4: The protein CENP-A in relation to the microtubule, kinetochore and centromeric DNA (figure modified from Burrack et al., 2011).

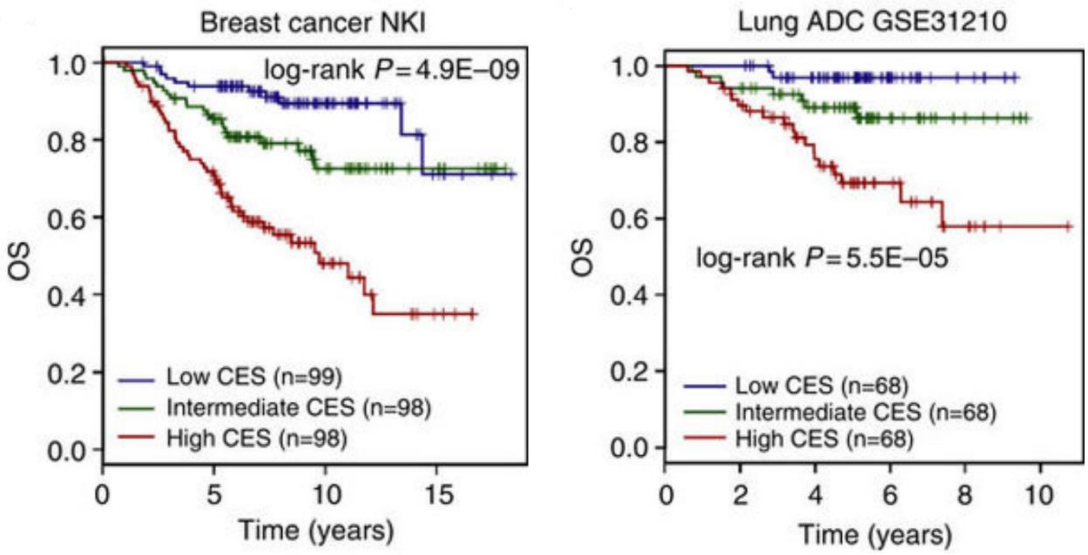

Figure 5: Kaplan-Meier survival curves for two analyzed sets of cancers split into high (red), intermediate (blue) and low (green) groups based on CES score. Overall survival (OS) is shown over time (figure modified from Zhang et al., 2016).

Studies from human cells have shown that when *CSE4* (the gene for CENP-A) is overexpressed, cells experience CENP-A mis-localization and the protein is seen in non-centromeric regions of the DNA (Shrestha et al., 2017). Further, this overexpression and mis-localization results in chromosome segregation errors and CIN. These cells also have weakened native kinetochores, which contribute to the CIN phenotype. Interestingly, the number of chromosome segregation errors and CIN can be reduced in these cells by correcting the mis-localization of CENP-A. Studies on CENP-A binding domains in chromosomes show that the amount of CENP-A bound is proportional to the length of the alpha-satellite DNA (highly repetitive region around centromeres) (Sullivan et al., 2011). Although the amount of CENP-A bound varies between individuals and chromosomes, the proportion of bound CENP-A to alpha-satellite DNA always remains the same. In cancer-like cells, increased length of alpha satellite DNA regions are seen correlated to increased levels of bound CENP-A. Studies from colorectal cancers show that excess CENP-A arising from overexpression will localize to non-centromeric regions of the DNA and

contribute to CIN (Athwal et al., 2015; Tomongata et al., 2003). Taken together, this suggests the CENP-A overexpression and the mis-localization that results can drive the CIN phenotype.

When *CSE4* is overexpressed in *Candida albicans*, a yeast model organism, we see increases in centromere-specific nucleosomes, kinetochore proteins and microtubule attachments per centromere compared to control cells (Figure 6B) (Burrack et al., 2011). Interestingly, although these data suggest CIN that may lead to aneuploidy, chromosome loss is not seen in the *CSE4/*CENP-A overexpressing *C. albicans.* In this study, the location of CENP-A binding remains at the centromere even upon overexpression of the protein, as revealed through chromatin immunoprecipitation (ChIP) (Figure 6A from Burrack et al., 2011). Although the location of binding does not change, the overall amount of CENP-A bound is seen increased in the *CSE4/*CENP-A overexpressing *C. albicans* (Figure 6A). Although *CSE4/*CENP-A overexpression alone does not result in aneuploidy in human or yeast cell experiments, the CIN observed may prime cells for aneuploidy and potentially the development of a cancer phenotype.

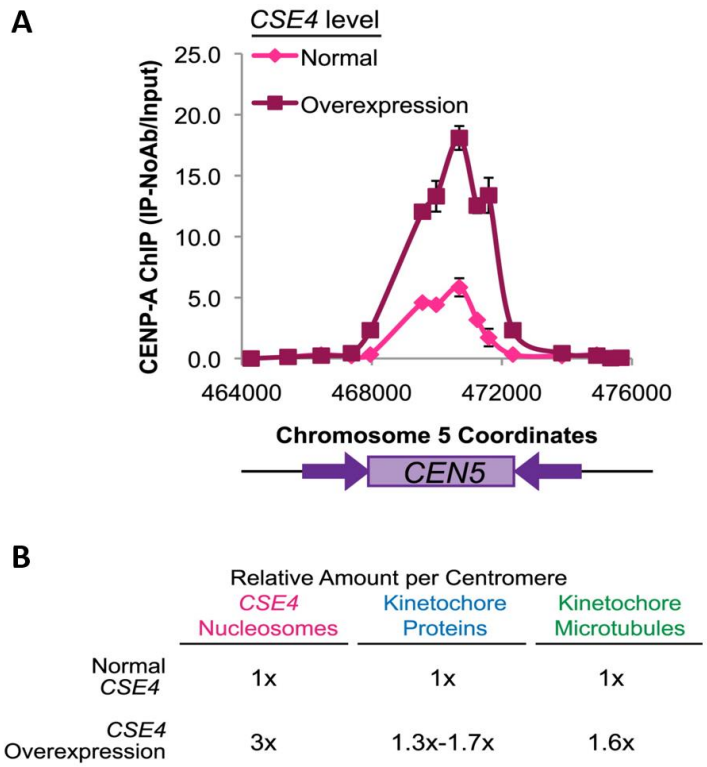

Figure 6: CENP-A binding location under *CSE4/CENP-A* wildtype expression and overexpression in *C. albicans* does not differ and remains localized around the centromere (A). *CSE4/CENP-A* overexpression increases the number of nucleosomes, kinetochore proteins and kinetochore microtubules recruited (B) (figures modified from Burrack et al., 2011).

Combinatory effects of altered cancer genes that cause CIN

It is known that *CSE4/*CENP-A overexpression in combination with other mutations can result in aneuploidy. In Shrestha et al. (2017), the mutations in the cancer cell lines HeLa and RPE1 along with *CSE4*/CENP-A overexpression was able to cause lagging/mis-segregation of chromosomes. Previous data suggest that overexpression of *CSE4/*CENP-A with a checkpoint gene alteration may be a mechanism that would result in aneuploidy. When Retinoblastoma protein (pRB) is knocked down with an siRNA targeting *RB* in human colon cancer cells, the result is chromosome instability (Figure 7 modified from Amato et al., 2009) and increased levels of *CSE4*/CENP-A (Amato et al., 2009). When pRB levels and *CSE4*/CENP-A levels were knocked down simultaneously (using two siRNA's targeting *RB* and *CSE4*), a phenotypic recovery was seen from the pRB knockdown cells. One biomarker of chromosome instability

is the formation of micronuclei, which are small chromosomal fragments that fail to be incorporated into one of the daughter cells during cell division. In the *RB* knockdown cells, about 30% of cells had micronuclei compared to 10% of cells with *RB* and *CSE4*/CENP-A knockdown (Figure 7). Thus, *CSE4*/CENP-A overexpression likely caused some of the chromosome instability that lead to the micronuclei formation. In this study, *MAD2* was also seen overexpressed, but changes in the spindle assembly complex were not seen. The *MAD2* levels were strongly correlated with levels of *BRCA1*, a regulator of *MAD2*. When *BRCA1* levels were altered in the cell, corresponding changes were seen in *MAD2*. Thus, the increased *MAD2* was attributed to *BRCA1* level increase after pRb depletion.

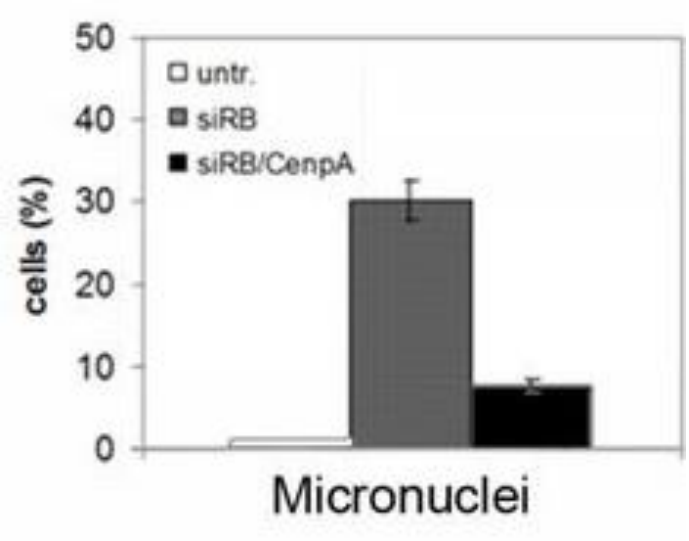

Figure 7: In control cells (untr.), no micronuclei were seen. When pRB levels are knocked down (siRB) After *CSE4*/CENP-A overexpression is knocked down with an siRNA targeting *CSE4*, percentage of cells with micronuclei is significantly decreased when compared to percentage of cells with micronuclei after pRB knockdown with an siRNA targeting *RB* (figure modified from Amato et al., 2009).

Alternative Hypothesis

Although a correlative relationship exists between *CSE4/CENP-A* and *MAD2* and cancer formation, it may not be causal. An alternative proposal argues that all kinetochore genes are upregulated together due to activation of a cell division program in cancerous cells. In other words, *CSE4/CENP-A* and *MAD2* overexpression may be a result of aneuploidy/cancer phenotypes rather than a driver for it. The cell

division proteins that are interrelated may work together to progress the disease. One study analyzed gene expression from over 3,000 cancer cell lines and saw that kinetochore genes are coordinately regulated within samples. For example, *MAD2* and its downstream target, *CDC20* were correlated with a value of 0.43 in one dataset and 0.85 in another. The study concluded that the coordinate upregulation can be attributed to the forkhead transcription factor *FOXM1*, but that individual proteins are not mechanistically important as a driver mechanism for cancer development (Thiru et al., 2014).

Pharmacogenomics

Pharmacogenomics is the study of how drug respnses differ in different genetic variants (Aneesh et al., 2009). The drug response under a certain condition can illuminate genetic differences and help researchers determine how these genetic differences contribute to the cell's phenotype. This technique can be used to study our genes of interest, *MAD2* and *CSE4*/CENP-A. Previous studies have identified thousands of gene-drug interactions that can be used to identify compounds that will interact with a gene or protein of interest to study its function. With advancements in bioinformatics and genetic sequencing, these tools are becoming even more powerful today. In 1999, 54 papers on

Spelunking in Cyberspace

Electricity brings the answer
to scientific schematics
The technical chaos an excavation site
with location unknown
You don't know if you are digging
At Qumran or in a sandbox
with nothing but tiny grains
varying in shades of light brown

The white screen glows and the cave crawl begins
You keep your head up and you sift through the data
Your headlight shines only on one location
so keeping still is not an option
You venture onward- illuminating and enlightening
laying the blueprint for the future

pharmacogenomics were published and since 2003, over 300 papers per year on the topic have been published. These studies utilize drugs and compounds to reveal genetic information that was previously unknown. In a pancreatic cancer study, DNA damaging drugs were used to reveal PalB2 as a new personalized cancer therapeutic target (Villarroel et al., 2011). Here, studied *MAD2* and *CSE4*/CENP-A in the presence of compounds that specifically target their functions. For our pharmacogenomics analysis we used publicly available databases. We first used the STRING database (Szklarczyk et al., 2017) to determine the protein-protein interaction networks of MAD2 and *CSE4*/CENP-A. STRING contains known and computationally predicted protein-protein interactions using lab experiments, conserved co-expression, genomic predictions, automated text-mining and other databases to curate information. These protein networks were used to find potential compounds that interact with MAD2 or *CSE4*/CENP-A through the Comparative Toxicogenomic Database (CTD) (Davis et al., 2016). The CTD gathers information from MEDLINE and PubMed about interactions between chemicals and genes/proteins and specifies the interaction type. The identified compounds from the analysis were then used to study MAD2 and *CSE4*/CENP-A.

Goal and Hypothesis

The main goal of this honors thesis is to explore whether dysregulation of *CSE4/CENP-A* and *MAD2* is a consequence of the cancer phenotype or a driver for it. To determine this, *CSE4/CENP-A* is overexpressed when *MAD2* is deleted and when *MAD2* is expressed at normal levels in *C. albicans* and CIN and aneuploidy are examined. Although data shows that high levels of both *MAD2* and *CSE4*/CENP-A overexpression can be used to predict tumor severity and survival probability (Zhang et al., 2016), a bioinformatical analysis (R2 database, http://r2.amc.nl) shows that low levels of *MAD2* and high levels of *CSE4*/CENP-A can also be a predictor for poor survival probability. As shown in colon cancer Kaplan Meier curves (Figure 8), deaths are significantly higher with low levels of *MAD2* ($p=2x10^{-6}$) and high

levels of *CSE4*/CENP-A ($p=4.4x10^{-4}$) compared to samples that expressed *high* MAD2 and low *CSE4*/CENP-A (Sample: core transcript, Sveen, 333 samples, rma sketch- huex10t). Similar results are seen in B-cell lymphoma (Xiao, 420 samples, fRMA- u133p2) where higher death rate is seen correlated to low levels of *MAD2* (p=0.048) and high levels of *CSE4*/CENP-A ($p=4.4x10^{-4}$). In *C. albicans*, the complexity and mechanism of *MAD2* is conserved from humans to yeast, where the O and C-MAD2 conformers are also necessary for function in yeast (Nezi et al., 2006). This conservation validates the study of *MAD2* dysregulation using *C.albicans* and allows results to be more applicable to humans. A *C. albicans* strain with *MAD2* knocked out (homozygous null) is transformed with an inducible *CSE4*/CENP-A promoter. This strain, along with wildtype *C. albicans* strain with the inducible *CSE4*/CENP-A will be tested against drugs identified to target *MAD2* and *CSE4*/CENP-A. Growth assays and chromosome loss will be examined for the yeast strains with the compounds of interest to gain insight into the mechanism of *MAD2* and *CSE4*/CENP-A dysregulation.

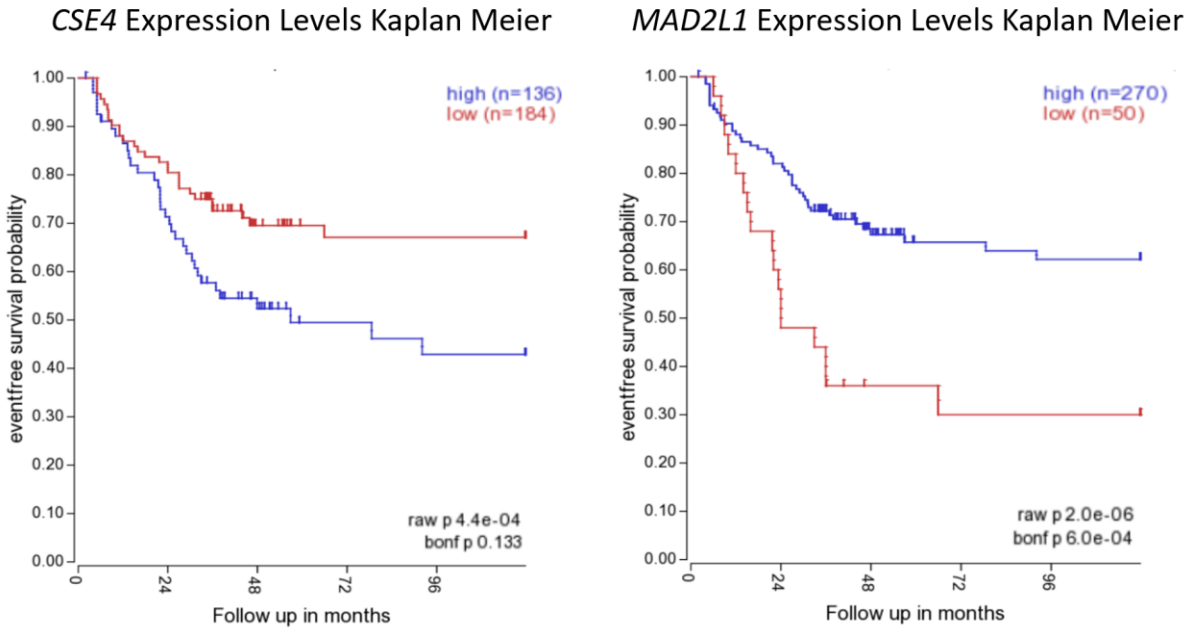

Figure 8: Colon cancer Kaplan Meier curves for *CSE4*/CENP-A expression levels (left) and *MAD2L1* expression levels (right). Data obtained from R2 database (Sample: core transcript, Sveen, 333 samples, rma sketch- huex10t).

Methods

Strain construction and growth conditions

To alter CENP-A levels, an existing strain of *C. albicans* with a *PCK1-CSE4* insert was used (Burrack et al., 2011). Growth of the strain in Yeast Extract-Peptone-Dextrose (YPA+glu) resulted in normal expression of *CSE4/*CENP-A while growth in Yeast Extract-Peptone-Succinate (YPA+succ) overexpressed *CSE4*/CENP-A. The *PCK1-CSE4* construct was also cloned into a *C. albicans MAD2* deletion strain through a lithium acetate transformation as previously described (Burrack et al., 2016). A URA3 selectable marker on the insert confirmed transformation success through plating on Synthetic dextrose complete (SDC)-URA plates. This allowed for the exploration of altered CENP-A levels without the presence of *MAD2* using MAD2del/*PCK1_CSE4*.

Helical twists run
bands glowing vibrant colors
lines will tell the fate

Confirmation of insertion and expression

To confirm the insertion of the *PCK1-CSE4* construct, a check PCR was performed on MAD2del/*PCK1_CSE4* colonies from SDC-URA plates. Genomic DNA was prepared with phenol chloroform extraction and PCR primers designed to span the region between the insertion and *CSE4* were used. *Taq* PCR was performed and agarose gel electrophoresis was used to determine the product size and confirm proper insertion. Gene expression levels of *CSE4* were confirmed with quantitative RT-PCR. Strains were inoculated in YPA+glu at 30°C overnight and diluted (1:100) into induction (YPA+succ) and repression (YPA+glu) medias for 5-6 hours. RNA was purified using MasterPure Yeast RNA Purification Kit (Epicentre) in accordance with manufacture instructions and treated with DNase (Epicentre) to remove genomic DNA contamination. Purified RNA was resuspended in Tris-EDTA (TE) buffer with Riboguard RNase inhibitor and the ratio of absorbance at 260/280nm confirmed the purity

of the sample. From the RNA, cDNA was synthesized with the ProtoScript First Stand cDNA Synthesis Kit according to manufacture instructions. The cDNA and RNA samples were run with Luna Universal qPCR Master Mix (NEB) according to manufacturer's instructions with forward and reverse primers for *TEF1* (F:aataccacgttaccgtcattgat, R: ccagtgatcatattcttgatgaaatc), *PCK1* (F:cgaatccacctcatccataac, R:tctagttctcaagtaatccaaagctc) and *CSE4* (F:tggcaagactttcaggacaa, R:cctctgcacttgttccttgg). Sample mRNA levels were quantified with the Qiagen Rotor-Gene cycler according to manufacturer's instructions and $\Delta\Delta C^T$ was used to determine the relative expression of mRNA levels while correcting for primer efficiencies.

Compounds identified for Pharmacogenomic exploration

The STRING database was used to determine protein-protein interaction networks of Mad2 and CENP-A in *S. cerevisiae* and *Homo sapiens*, as *C. albicans* interactions were not available (Szklarczyk et al., 2017). Interactions between proteins were direct (such as a physical interaction), regulatory, molecular or biochemical. From STRING, we examined only evidence from experiments and databases and set a minimum interaction confidence score of 0.95. The nature of each interactions (activating or inhibitory) was noted. Proteins identified were defined as being on the "axis" of Mad2 or CENP-A. To ensure results were applicable to our study, we confirmed that proteins on the "axis" had homologs in *C. ablicans.* The Comparative Toxicogenomic Database (CTD) (Davis et al., 2016) was used to identify compounds that inhibited *MAD2*, *CENP-A* or any member of their "axis". Interactions in all species were considered for this portion of the analysis. Leading compounds were compared to NCI60 Cancer Microarray Project Data (Scherf et al., 2000) which is composed of about 43,000 small molecules screened against 60 cancer cell lines. The NCI60 data was used to plot cancer cell line mRNA expression level of *CSE4* or *MAD2* against drug

Silico questions
Keys struck deliberately
Blueprint by IT

activity and no significant trends were identified. Compounds were scored based on the number of "axis" members they inhibited and if they directly inhibited *MAD2* or *CENP-A.* Five top compounds were selected for future study and purchased, Bisphenol A (BPA), Fulvestrant, Dasatinib, Cyclosporine and Sodium Arsenate (Sigma Aldrich, CAS #: 80-05-7, 129453-61-8, 302962-49-8, 59865-13-3, 10048-95-0 respectively). Compound selections were also based on price and safety of the chemicals.

Growth Analysis

Growth curves were performed by monitoring absorbance at 600nm for 24 hours. A Tecan Sunrise absorbance microplate reader with Tecan's Magellan software was used to collect data. Growth curves were performed on *MAD2*del/*PCK1_CSE4* and *MAD2*(wt)/*PCK1_CSE4* in YPA+succ or YPA+glu and with 0.25mM BPA, 50uM Fulvestrant, 60mM Dasatinib, 40uM Cyclosporine and 4mM Sodium Arsenate. For experimentation, Fulvestrant, Dasatinib and Cyclosporine were dissolved in DMSO, Sodium Arsenate in water and BPA in 10% ethanol. For each trial, four biological replicates were performed, and values were averaged to obtain a single growth curve. For analysis, logistic growth was assumed, and maximum population and growth rate determined for each trial (see math modeling of growth for further details). From the growth curve results, Fulvestrant and BPA were selected for further investigation.

Freezing cells, thaw out
Scorched post data collection
Disorder increase

Math modeling of growth

In our analysis of yeast growth, we determined the carrying capacity (K) and the maximum rate of growth (r). We initially obtained the carrying capacity by taking the maximum culture density and the growth rate by taking the slope at the inflection point of the logistic growth curve. This method of analysis was used for all growth assays. To further improve the statistical and computational methods

for comparing growth curves, additional methods were developed. For logistic growth, the change in population (P) over time (t) can be represented by the differential equation:

$$\frac{dP}{dt} = rP(1 - \frac{P}{K}) \qquad \text{eq.1}$$

where r is the maximum growth rate and K is the carrying capacity of the environment the yeast live in. The values of r and K in equation 1 are the same as the values of r and K from our initial analysis determined by taking the inflection point slope and maximum culture density. The solution to differential equation (eq.1) is as follows:

$$\begin{aligned}
\int \frac{dP}{P(1-\frac{P}{K})} &= \int r dt \\
\int \frac{dP}{P} + \int \frac{dP}{K-P} &= \int r dt \\
ln|P| - ln|K-P| &= rt + C \\
ln\left|\frac{K-P}{P}\right| &= -rt - C \\
\left|\frac{K-P}{P}\right| &= e^{-rt-C} \\
\frac{K-P}{P} &= e^{-rt-C} \\
P(t) &= \frac{K}{1+e^{-(rt+C)}}
\end{aligned} \qquad \text{eq.2}$$

Thus our growth curves that model population (P) over time (t) can be fit to equation 2 and parameters K, r and C determined. The experimental data was fitted to equation 2 in R using the non-linear least squares method. Interpretation of parameters K and r have been described and previously determined, but values for C were not calculated in our initial analysis.

To interpret C, notice that at the starting time point (when time is 0), the function is:

$$P(0) = \frac{K}{1 + e^{-C}} \qquad \text{eq.3}$$

So we can see that:

$$e^{-C} = \frac{K - P(0)}{P(0)} \qquad \text{eq.4}$$

Equation 4 shows that C is a function of our initial population value P(0) and carrying capacity K. Since we started with the same amount of yeast for each trial and the carrying capacity was constant within medias (YPA+glu or YPA+succ), we can interpret C as a "lag parameter", or a measure of when yeast growth occurs. To demonstrate this, Figure 9A shows the effect of changing C with constant values of K and r. Figure 9B shows data from two of our yeast growth assays fit to the logistic growth model. Values of C for each curve are shown, exhibiting how C can be interpreted as the "lag effect".

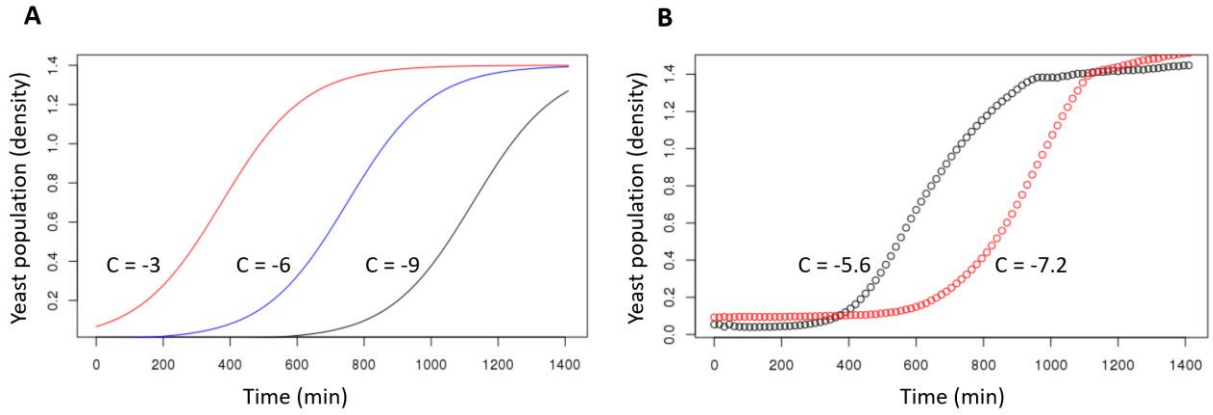

Figure 9: Logistic growth curves are simulated and plotted with varying values of "C" while "K" and "r" are held constant (K=1.4 and r=0.008) (A). Example growth assay data is shown and parameters obtained for "C" are noted for each curve to visualize how this parameter might be applied (B).

Fluctuation analysis

5-Fluoroorotic Acid (5-FOA) assays were performed to determine chromosome loss rate and aneuploidy as previously described (Spell and Jinks-Robertson, 2004). Cells grown in the presence of the drug 5-FOA (Gold Biotechnology) will die in the presence of URA3, which our strains possess. Thus, strains will die unless incorrect cell division occurs and URA3 is lost. Fluctuation analysis is used to quantify loss rates of *URA3* and chromosome loss. For the *MAD2*del-*PCK1_CSE4* strain, eight colonies are inoculated in 1ml YPA+glu or YPA+succ for 16-18hr at 30°C with shaking. Additionally, tests are performed in the presence of 0.25mM BPA and 50uM Fulvestrant. Cultures are diluted and plated on YPA+glu plates for colony counts (1 day incubation) and SD+5-FOA plates (3 day incubation) at 30°C. The median number of colonies per condition (Lea and Coulson, 1949) were used to calculate the 5-FOA resistance of the strains using methods previously described (Spell and Jinks-Robertson, 2004).

Results

Using pharmacogenomics as a system to study altered levels of MAD2 and CENP-A expression

To explore alteration of *MAD2* and *CSE4*/CENP-A, we took a pharmacogenomic approach. To do this, compounds were identified that would potentially downregulate the proteins in vivo. Protein-protein interactions can be direct (through mechanisms such as physical contact or binding) or indirect (through mechanisms such as biochemical or translational changes). These interactions are essential for functional cellular processes and thus were explored in an attempt to disrupt Mad2 and CENP-A function. The STRING database identified proteins that interacted with MAD2 and CENP-A in *S. cerevisiae* and *Homo sapiens* (Szklarczyk et al., 2017). Proteins in the "axis" of MAD2 and CENP-A are shown in Figure 10. Since *C. albicans* would be used for experimentation, NCBI's HomoloGene and Candida Genome Database were used to identify genes conserved in *C. albicans* to be included in the axis'.

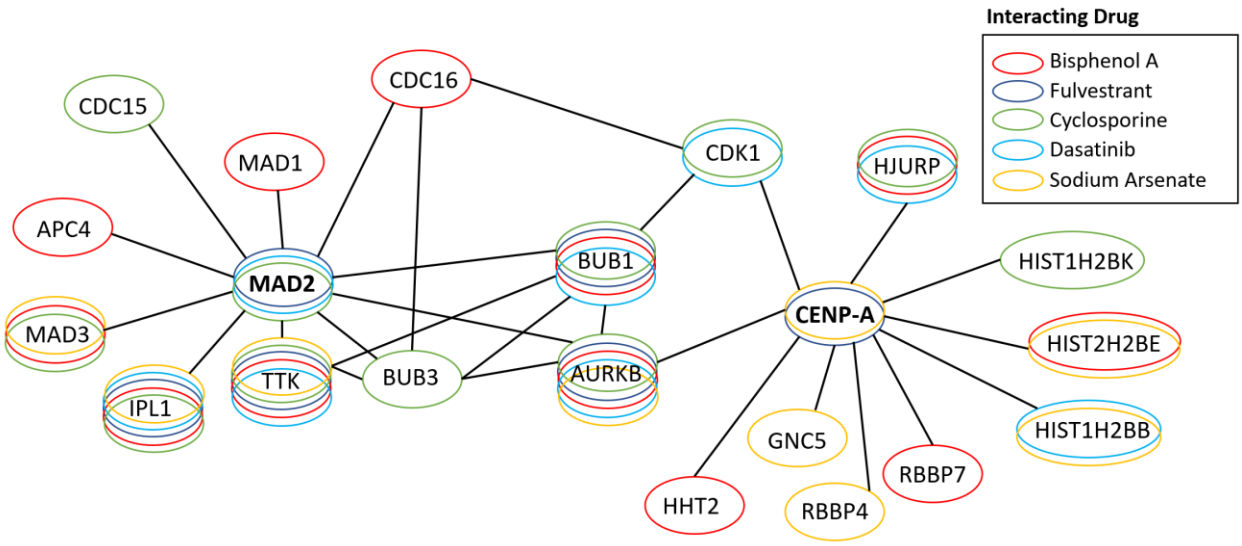

Figure 10: A diagram showing the Mad2 and CENP-A network of interacting proteins. Interactions were determined using the STRING database for human data sources with 95% confidence. The drugs that have been shown to affect the network members and downregulate MAD2 and CENPA are shown as colored circles on the diagram.

	MAD2	MAD2 network (# of nodes inhibited)	CENP-A	CENP-A network (# of nodes inhibited)
Fulvestrant	X	4	X	2
Bisphenol A		8		7
Dasatinib	X	4		6
Cyclosporine	X	8		6
Sodium Arsenate		4	X	6
Valproic Acid		6		6
Dibutyl Phthalate		8		5
Tretinoin		4		5
Copper Sulfate	X	5		3
Testosterone		5		5
Cisplatin	X	2	X	2

Figure 11: The drugs that were top hits in the bioinformatic search and interfere with Mad2, CENP-A or a network member's gene products.

We used the Comparative Toxicogenomic Database (CTD) (Davis et al., 2016) to look up compounds that interacted with *MAD2*, *CSE4*/CENP-A or proteins on their axis' to inhibit *MAD2* or *CSE4*/CENP-A. Compounds were compared to NCI60 Cancer Microarray Project Data (Scherf et al., 2000) which is composed of about 43,000 small molecules screened against 60 cancer cell lines. The mRNA expression levels of *CSE4* and *MAD2* were plotted against drug activity for each cell line, but no significance was found. This further confirmed that there were no previously known results relating the protein to the compound in cancer cells and thus the compound was worth exploring. The top compounds were identified as having the highest number of interactors inhibiting *MAD2* or *CSE4/*CENP-A (Figure 11). Five of the top compounds were purchased for future investigation, Bisphenol A (BPA), Fulvestrant, Dasatinib, Cyclosporine and Sodium Arsenate.

Construction of inducible C. albicans and growth assays performed on strains identified BPA and Fulvestrant for future study

A *C. albicans MAD2* deletion strain (*MAD2*del) was transformed with a *CSE4/*CENP-A promoter to become *MAD2*del-*PCK1_CSE4*. We confirmed overexpression with qRT-PCR and found *CSE4* was overexpressed at least 5-fold in all trials. The *MAD2*del-*PCK1_CSE4* strain and a previously constructed strain that expressed normal *MAD2* with the *PCK1_CSE4* promoter (*MAD2*normal-*PCK1_CSE4*) were used in growth assays to analyze four trials of *C. albicans* differentially expressing *MAD2* and *CSE4/*CENP-A. The *MAD2*normal-*PCK1_CSE4* grown in YPA+succ produced "Mad2-normal/CENP-A-overexpressed" and grown in YPA+glu produced "Mad2-normal/CENP-A-normal". Similarly, *MAD2*del-*PCK1_CSE4* grown in YPA+succ produced "Mad2-del/CENP-A-overexpressed" and grown in YPA+glu produced "Mad2-del/CENP-A-normal".

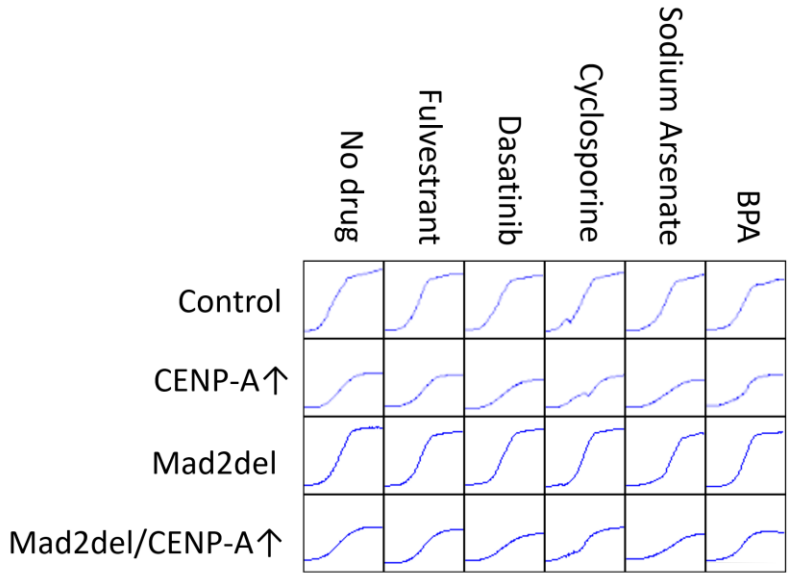

Figure 12: A representative figure showing growth curves for the drug treated *C. albicans* strains differentially expressing *MAD2* and *CSE4*/CENP-A. Growth assays were performed over 24 hour periods and culture density was used to measure *C. albicans* population size. BPA and Fulvestrant were selected for differentially affecting the growth rate of yeast in Mad2del/CENP-A↑ without evidence of too much toxicity to the cells (seen with Cyclosporine) or affecting the total growth amount (seen with Sodium Arsenate).

We performed growth assays in the five drugs selected for pharmacogenomic analysis. Figure 12 shows an example of the logistic growth curves produced from growth assays. From the curves, the final density of the cultures was measured and compared across strains and conditions. Across all conditions, the CENP-A/*CSE4* overexpressed cells had lower final culture densities. This was due to the growth in YPA+succ, which was used to overexpress CENP-A/*CSE4*, but resulted in slower *C. albicans* growth compared to YPA+glu. Final culture densities did not differ significantly within medias.

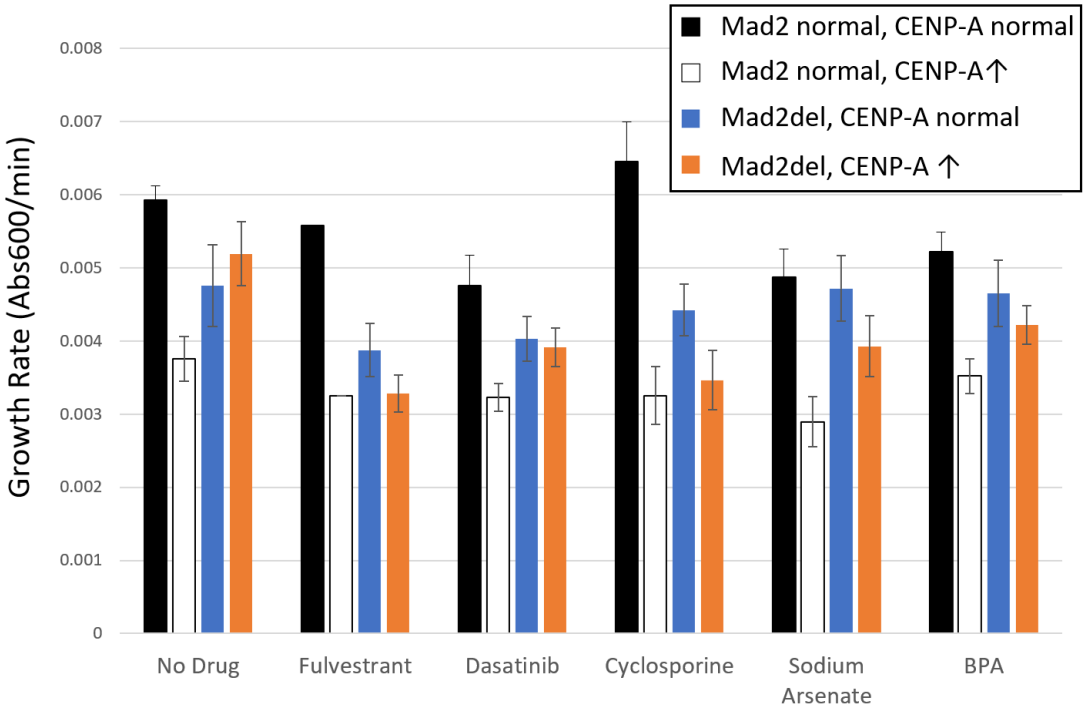

Figure 13: Mean growth rates for *C.albicans* strains treated with drugs for various expression conditions with standard error bars shown (n=1-7). Strains were grown for 24 hours in YPA with glucose or succinate and either no drug, 0.5mM BPA, 50uM Fulvestrant, 60mM Dasatinib, 40uM Cyclosporine or 4mM Sodium Arsenate. Absorbance levels were recorded to measure culture population and the growth rate was measured as the rate of change at the inflection point of the logistic growth curve for each trial.

We assumed logistic growth to determine the growth rate for each assay (Figure 13). A two-way ANOVA test showed no significant differences that were not due to media effects. For the wildtype (WT) strain (Mad2-normal/CENP-A-normal), the mean growth rate with no drug was 0.0059 Abs600/min and drug treatment means ranged from 0.0048 to 0.0064 Abs600/min. We saw that all growth rates for the drug treated WT strains were lower than the no drug control except for in Cyclosporine, where we saw a rate of 0.0064 Abs600/min. For the Mad2-normal/CENP-A-overexpressed strain, the mean growth rate with no drug was 0.0038 Abs600/min. Treating the strain with drugs produced mean growth rates that ranged from 0.0029 to 0.0035 Abs600/min. The Mad2-del/CENP-A-normal strain with no drug had a mean growth rate of 0.0048 Abs600/min and drug treatment of the strain produced rates ranging from

0.0039 to 0.0047 Abs600/min. Finally, the Mad2-del/CENP-A-overexpression strain mean growth rate with no drug was 0.0052 Abs600/min and drug treatment rates ranged from 0.0033 to 0.0042 Abs600/min. For all drugs treatments, the same pattern was seen for strain's mean growth rates. The highest growth rate was seen in the Mad2-normal/CENP-A-normal strain, followed by the Mad2-del/CENP-A-normal strain, then the Mad2-del/CENP-A-overexpressed strain and the Mad2-normal/CENP-A-normal, which had the lowest growth rate.

We chose to focus further study on drugs that seemed to differentially affect strains rather than just kill cells. Based on preliminary experiments, Fulvestrant and BPA were chosen for further exploration. Although Dasatinib appeared to decrease the growth rates of the strains, it affects both the Mad2-del strains equally, which was not the differential expression we were interested in. With Cyclosporine treatment, the growth rates produced were higher than WT strain treated with no drug. This, along with examining the shape of the growth curves, suggests that logistic growth was not followed and thus analyzing these data would likely be difficult. Similar to Dasatinib, Sodium Arsenate did not appear to have a differential effect on the growth rate of cells in strains with normal CENP-A levels (Mad2-normal/CENP-A-normal and Mad2-del/CENP-A-normal). With BPA treatment, deleting *MAD2* slightly lowered the growth rate, but deleting *MAD2* in the presence of CENP-A overexpression slightly increase the growth rate. For Fulvestrant, relatively equal growth rates were produced for both *MAD2* deletion strains (with and without CENP-A overexpression).

After we collected preliminary data, further trials were run on the selected drugs, BPA and Fulvestrant. The individually plotted growth rates for no drug, BPA and Fulvestrant treated strains are shown in Figure 14. This figure shows the variability in the data, which had more noise than we expected. Letter codes in Figure 14 show the significance between the treatment groups, where a significant difference

between conditions exists if their codes do not share a letter. For example, WT BPA and WT no drug cells had a significantly higher growth rate than MAD2-normal/CENP-A-overexpression treated with both Fulvestrant and BPA. The WT no drug and BPA trials were also significantly greater than the MAD2-del/CENP-A-overexpression strain treated with Fulvestrant. The MAD2-del/CENP-A-overexpression strain treated with Fulvestrant had the lowest growth rate and was significantly lower than the no drug condition for the same strain. Additionally, it had a significantly lower growth rate than the MAD2-del/CENP-A-normal in no drug and BPA conditions as well as the MAD2-normal/CENP-A-normal in no drug and BPA.

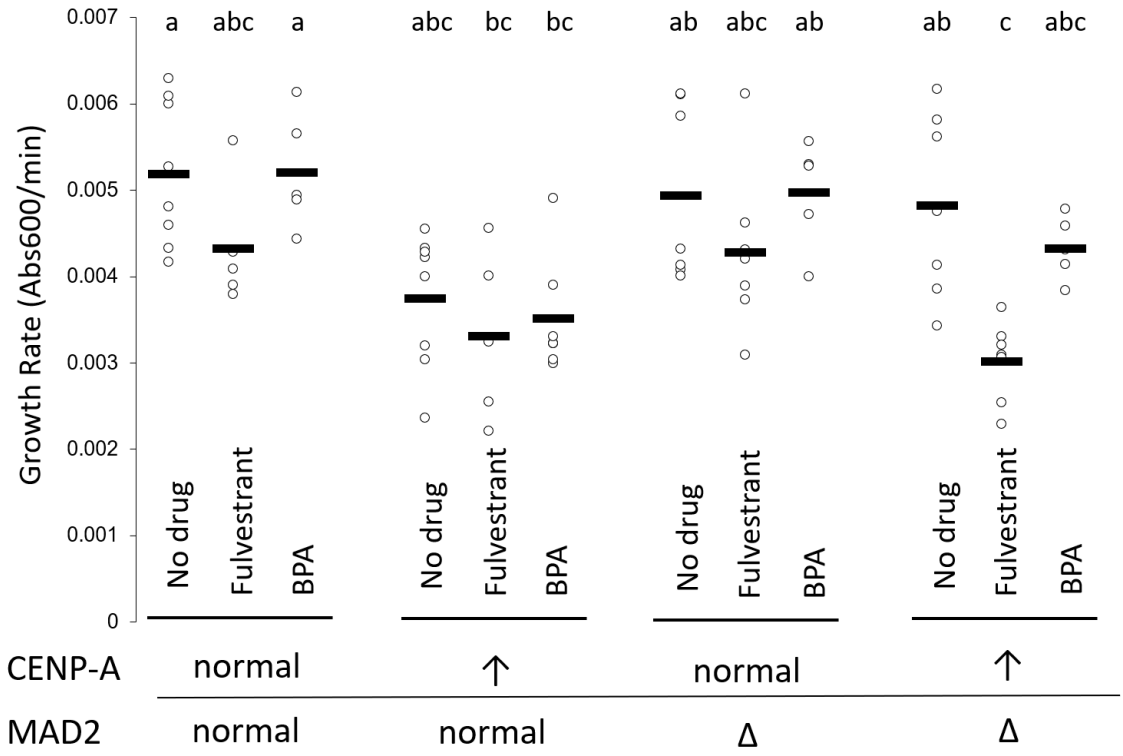

Figure 14: Growth rates for *C.albicans* strains treated with estrogenic drugs Fulvestrant and BPA. Strains were grown for 24 hours in YPA with glucose or succinate and either no drug, 50uM Fulvestrant or 0.25mM BPA. Absorbance levels were recorded to measure culture population. The growth rate was measured as the rate of change at the inflection point of the logistic growth curve for each. A two-way analysis of variance test (ANOVA) was performed with Tukey's post-hoc test (confidence level 0.95) and significance letter codes are shown above each condition. Common letters between conditions indicated no significant difference between the conditions (n=5-8).

Mathematical model fitting of growth curves produces an additional lag period parameter

Growth assay data from the trials shown in Figure 14 were fit to a mathematical model to determine growth rate (r), carrying capacity (K) and an additional parameter (C) that was interpreted as a measure of the "lag" of the culture. Mathematically computed values will be designated r_{model} and K_{model} to differentiate them from initially computed values of r and K. Values obtained for r_{model} (Figure 15) appear to follow a similar pattern as values for r in Figure 14. This pattern reflects the media effects between glucose and succinate. Since glucose is a more favorable media source, the strains expressing CENP-A at normal levels had higher growth rates. A two way ANOVA showed no significant differences outside of media effects for values of $r_{model.}$ The values of r_{model} were seen to be larger than the r values previously obtained. The mean r_{model} for the WT strain with no drug was 0.0095 Abs600/min and Fulvestrant and BPA means were 0.0085 and 0.0097 Abs600/min. For the MAD2-normal/CENP-A-overexpressed strain, the mean r_{model} with no drug was 0.0064 Abs600/min. Fulvestrant and BPA treatment of the strain produced mean r_{model} values of 0.0064 and 0.0067 Abs600/min. The MAD2-del/CENP-A-normal strain had a mean r_{model} of 0.0089 Abs600/min with no drug and values for Fulvestrant and BPA were 0.0088 and 0.0084 Abs600/min. Finally, the MAD2-del/CENP-A-overexpression strain's mean r_{model} value with no drug was 0.0071 Abs600/min and drug treatment values for Fulvestrant and BPA were 0.0062 and 0.0057 Abs600/min.

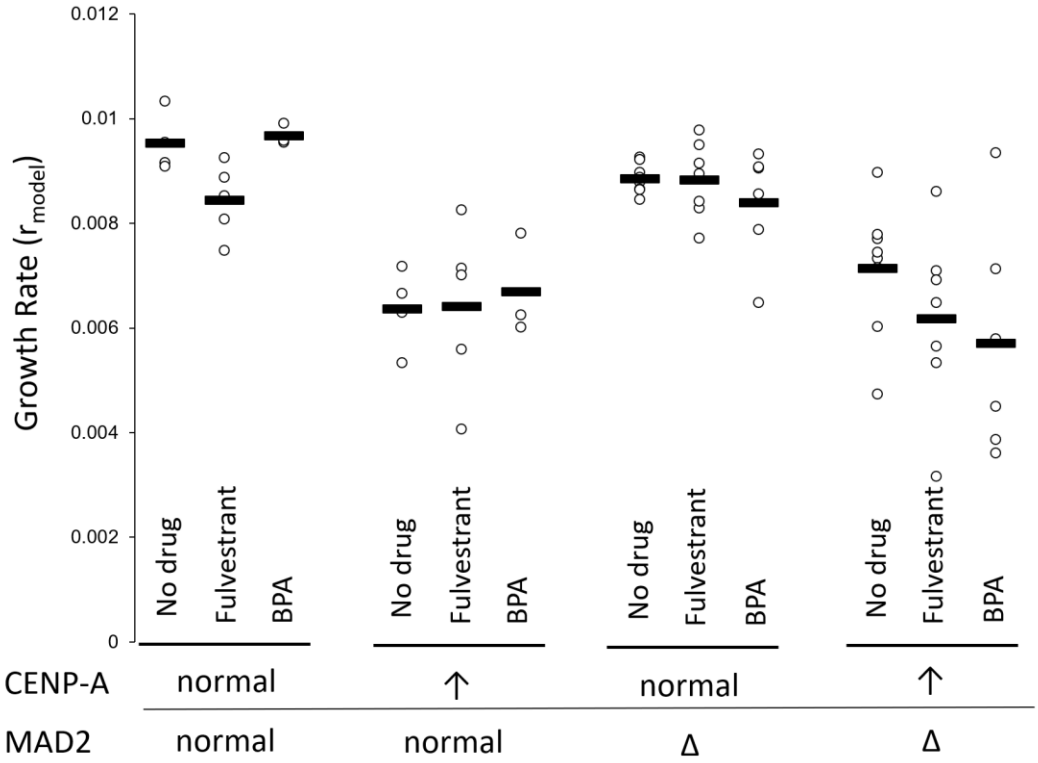

Figure 15: Results from growth curve data fit to a logistic growth model to obtain a growth rate (r_{model}). Rates from each trial are individually plotted (n=5-8) and mean rates are shown as a black bar. *C. albicans* strains were grown for 24 hours in YPA with glucose or succinate and either no drug, 50uM Fulvestrant or 0.25mM BPA and absorbance levels were recorded to measure culture population.

Values were also obtained for C in equation 2, which can be interpreted as a measure of culture's growth lag before the yeast reach maximum growth rate (r). As shown in Figure 9, more negative values of C shift the curve to the right and delay growth. C's are shown in Figure 16 and a two-way ANOVA showed no significant differences outside of media effects. The mean value of C for the MAD2-normal/CENP-A-normal strain (no drug) was -5.49 with Fulvestrant and BPA means were -5.86 and -6.10. For the MAD2-normal/CENP-A-overexpressed strain, the mean no drug C was 4.25 and treatment with Fulvestrant and BPA had C's of -4.74 and -4.89. The MAD2-del/CENP-A-normal strain (no drug) had a mean C of -6.10 and Fulvestrant and BPA treatment produced values of -6.59 and -5.75. Finally, the

MAD2-del/CENP-A-overexpression strain's mean C value with no drug was -5.26 and drug treatment values for Fulvestrant and BPA were -5.01 and -4.45.

Values for K obtained from the model did not have significant differences outside of media effects (determined with a two-way ANOVA). Additionally, low levels of variability within media types are seen for K values. Mean absorbance values for carrying capacity (K) of MAD2-normal/CENP-A-normal cells (grown in YPA+glu) ranged from 1.43 to 1.53. The other strain grown in YPA+glu, MAD2-del/CENP-A-normal, had mean K values from 1.49 to 1.53. The strains grown in YPA+succ had lower K values, with MAD2-normal/CENP-A-overexpression ranging from 1.01 to 1.09 and MAD2-del/CENP-A-overexpression from 1.02 to 1.20.

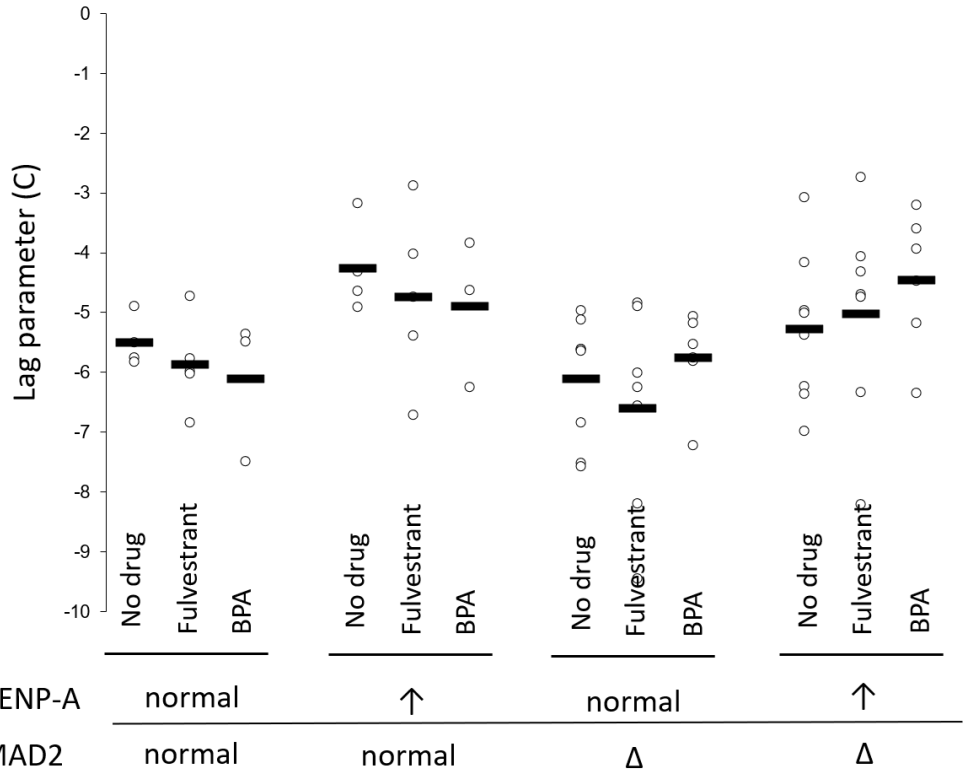

Figure 16: Results from growth curve data fit to a logistic growth model to obtain a lag parameter "C". Rates from each trial are individually plotted (n=5-8) and mean rates are shown as a black bar. *C. albicans* strains were grown for 24 hours in YPA with glucose or succinate and either no drug, 50uM Fulvestrant or 0.25mM BPA and absorbance levels were recorded to measure culture population.

Flux analysis shows low mutation rates and high variability in Mad2del cells

We next explored whether decreased growth rates were due to increased chromosome loss rates in cells. Figure 17 shows the chromosome loss rates from the flux assays. When in the no drug conditions, Mad2-del/CENP-A-normal cells had a median of 1.09×10^{-5} mutations/cell and the Mad2-del/CENP-A-overexpressed cells had a median of 7.98×10^{-6} mutations/cell. When treated with Fulvestrant, Mad2-del/CENP-A-normal cells had a median of 7.01×10^{-5} mutations/cell and the Mad2-del/CENP-A-overexpressed cells had a median of $2.70\text{x } 10^{-6}$ mutations/cell. In BPA, Mad2-del/CENP-A-normal cells had a median of 6.10×10^{-6} mutations/cell and the Mad2-del/CENP-A-overexpressed cells had a median of 2.50×10^{-5} mutations/cell. A two-way ANOVA showed no significance in the data between or within variables. Generally, CENP-A overexpression may slightly decrease mutation variability and mutation rate in cells treated with no drug and Fulvestrant. Additionally, BPA seems to have slightly higher mutation rates and variability for Mad2-del/CENP-A-overexpression cells. The raw colony count data was analyzed using the method of the median, but there seemed to be too many outliers for this to be an accurate representation of the data.

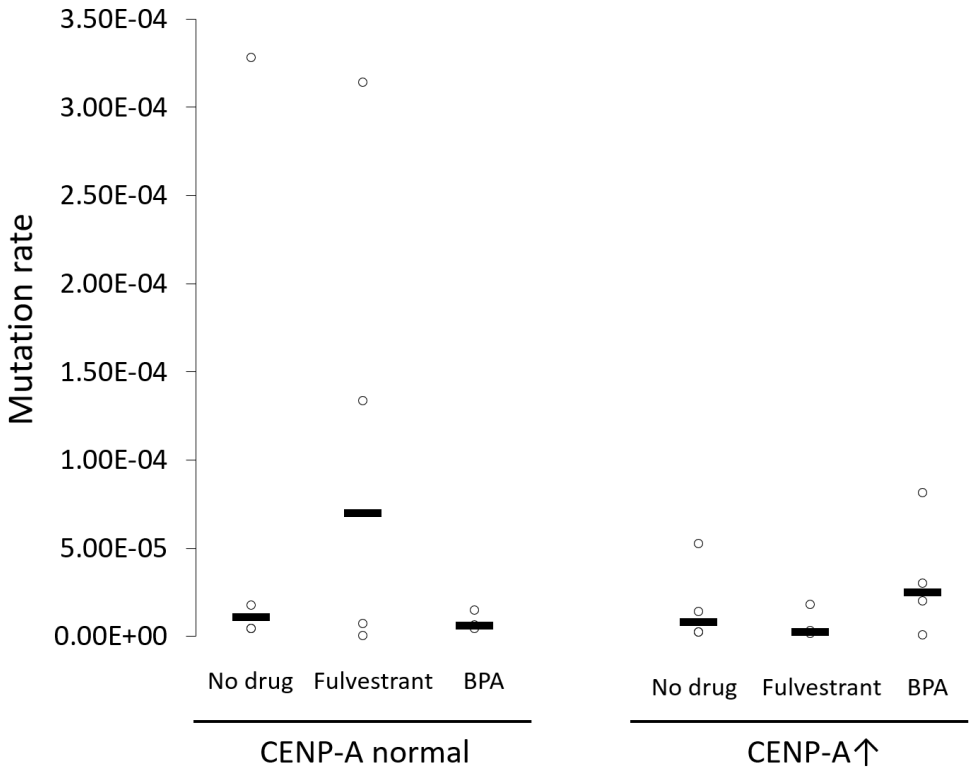

Figure 17: The effect of drug treatment on mutation rate in ΔMAD2 *C.albicans.* A 5-FOA assay is used to calculate *URA3* loss, which is representative of chromosome loss/aneuploidy. Strains are grown in YPA with glucose or succinate and either no drug, 50uM of Fulvestrant or 0.25mM BPA. ANOVA revealed no significant difference in mutation rates between groups (n=3-4).

closely packed structures

Copy machine broken

again, and it's left for days

Complaints, emails, power on and off

And a lot of coffee later

Finally fixed

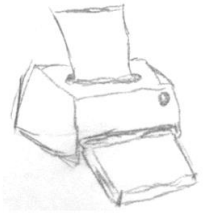

Copy machine broken

*again, and e*veryone is on their feet

Panic erupts, alarms are sounding, fear of the unknown, the uncontrolled

No time for coffee only cyclins and checkpoints

Finally fixed

Discussion

Compounds examined

To enhance our study of *MAD2* and *CSE4*/CENP-A, compounds were identified that would inhibit genes of interest as well as their "axis" of interacting proteins. To analyze how drug treatment affected Mad2 and *CSE4*/CENP-A in *C. albicans* strains, we will first investigate the drugs studied and their known mechanisms.

Fulvestrant has been shown to inhibit levels of *MAD2* and *CSE4*/CENP-A in breast cancer cells (Ghayad et al., 2009; Scafoglio et al., 2006). Additionally, Fulvestrant inhibits members of the MAD2 network (TTK, BUB1, AURKB, IPL1) and CENP-A network (BUB1, AURKB) (information obtained from CTD, Davis et al., 2016). This gene transcription is altered through Fulvestrant's endocrine antagonist properties. Fulvestrant is used as an endocrine treatment for hormone sensitive cancers, such as breast, pituitary, hypothalamus or prostate cancers. Clinically, Fulvestrant inhibits growth of ER-positive MCF-7 breast

cancer cells by 80% (Wakeling and Bowler, 1987). The drug has shown promise in many breast cancer phase 3 trials (both individually and in combination with other agents) and particularly with metastatic tumors (Nathan and Schmid, 2017). In cells, gene transcription is controlled by oestrogen, which binds to estrogen receptors (ER) and results in dimerization, nuclear localization and DNA binding to regulate transcription. As an antagonist of estrogen, Fulvestrant is a steroidal analogue of 16B-oestradiol and binds competitively with estrogen to ER. This binding inhibits transcriptional signaling and results in an unstable and non-functional complex, leading to the degradation of the ER protein and reduction of oestrogen signaling (Wardley, 2002). When our cells are treated with Fulvestrant, gene transcription is for *MAD2*, *CSE4*/CENP-A and their networks are decreased.

Although Bisphenol A (BPA) has not been shown to affect *MAD2* and *CSE4*/CENP-A levels in cells, it inhibits members of the MAD2 network (BUB1, CDC16, MAD1, MAD3, IPL1, APC4, AURKB, TTK) and CENP-A network (RBBP7, AURKB, AURKA, HJURP, HHT2, BUB1, HIST2H2BE) (information obtained from CTD, Davis et al., 2016). Thus, we can use BPA to alter processes that involve *MAD2* and *CSE4*/CENP-A and analyze data from that standpoint. The mechanism through which BPA affects gene transcription is similar to Fulvestrant, and exposure to BPA in vivo has been shown to affect cellular transcription levels (Moriyama et al., 2002; Wadia et al., 2013). BPA is a non-steroidal synthetic monomer that also binds the nuclear ER and has been classified as “endocrine disrupting” (Vandenberg et al, 2009). The compound has been shown to have both agonistic and antagonistic properties in human tissues depending on cell and receptor type (Moriyama et al., 2002; Kurosawa et al., 2002). Further study includes examining extent to which Fulvestrant and BPA affect mRNA levels of *MAD2*, *CSE4*/CENP-A and their networks members through qRT-PCR.

In addition to these drugs directly impacting levels of *MAD2*, *CSE4*/CENP-A and their networks members, it's possible that the drugs are affecting the cells in a way that induces tetraploidy (4N DNA rather than the typical 2N DNA). An example of this phenomenon in *C. albicans* is with the drug Fluconazole, which is an antifungal that interferes with sterol biosynthesis and affects cellular membranes in fungi (Morschhauser, 2002). In *C. albicans*, Fluconazole has been shown to induce an abnormal trimeras phenotype, which is where three cells (mother, daughter and granddaughter) are connected. This results in a high percentage of unstable aneuploid cells that can become drug resistant (Harrison et al., 2014). It may be possible that the Fulvestrant and BPA cause a phenomenon, where alteration of membrane integrity and fluidity can lead to tetraploidy in cells by altering cell cycle dynamics.

Growth Assays show high variability and expose media effects

To overexpress CENP-A with the *PCK1_CSE4* promoter, cells were grown in YPA+succ rather than YPA+glu, which is considered a more favorable media. The pattern in Figures 13-15 exposes this problem, where growth in succinate (Mad2-normal/CENP-A-overexpression and Mad2-del/CENP-A-overexpression) consistently results in lowered growth rates. While there is clearly a media effect, future exploration will focus on differentiating this from any true biological effects that may be present.

When growth rates are plotted as points (Figure 14), the variability of the data can be seen. Although we expect fluctuations due to natural variations in the data that cannot be controlled, there is more noise than expected, making data interpretation difficult. Fitting a mathematical model to the growth assay data to more accurately determine parameters and obtain an additional parameter C may be a way to alleviate this problem. Fitting the growth assay data to the solution of the logistic growth equation resulted in three model parameters ($r_{model.}$ K_{model} and C) that can be compared. This method for calculating growth parameter values is more methodical and statistically powerful than the previously

used methods of finding the inflection point and calculating the slope. The model produced r_{model} values that were larger than values obtained for r. Although these values should be equivalent, it is not surprising that they differ due to the noise and variation seen in the growth curves that likely interfered with the calculation of the slope at the inflection point (r). The non-linear least square model used to calculate r_{model} creates a "best fit" equation for the data aimed to minimize the distance from the equation to each of the points along the curve. This method of obtaining an r_{model} value is likely more robust and would be less affected by imperfect data than the slope calculation to get r. Thus, future analysis on growth curves that show high levels of noise or variation can be analyzed using r_{model} with the aim of increasing the accuracy of the growth rate calculated. Values of C did not show significant differences, thus the drugs did not appear to have significant "lag effects" on the yeast. The derived parameter C, can also be used in future comparative analysis to examine lag effects.

Potential collaboration of Mad2 and CENP-A in the cell cycle

In the control cells with no drug treatment, the double mutant cells (Mad2-del/CENP-A-overexpression) exhibit a growth rate similar to control cells (Mad2-normal/CENP-A-normal). These Mad2-normal/CENP-A-overexpression cells are grown in the same media as the Mad2-normal/CENP-A-overexpression cells, which had the smallest growth rate without drug treatment. This suggests that deleting *MAD2* in the presence of CENP-A overexpression may have a "rescue effect" on the growth rate of cells not treated with drugs. Figure 18 outlines the possible schematic: the CENP-A overexpression promotes increased unstable kinetochore attachments, which leads to slowed cell division and growth rate. When the checkpoint protein, *MAD2,* is deleted, the MCC will lack the MAD2 protein and binding to the APC/C will be decreased. Since MCC-APC/C binding inhibits anaphase entry in the presence of unstable attachments, decreased binding will result in premature anaphase entry and an increased growth rate.

In cells without drug treatment, this effect is enough to partially or fully recover the growth rate of the cells.

The growth rates seen in the initial (all drug) growth assays from Figure 13 was similar to results from the BPA and fulvestrant assays (Figure 14). For treatment with BPA or no drug, both figures show slight growth rate increases from Mad2-normal/CENP-A-overexpression cells to Mad2-del/CENP-A-overexpression cells. Fulvestrant treated cells in Figure 14 also followed earlier patterns observed, where Fulvestrant treated Mad2-del/CENP-A-overexpression cells had the lowest growth rate. Fulvestrant was the only drug we tested that inhibited both *MAD2, CSE4*/CENP-A and their respective networks. This along with the low growth rate in the double mutant strain suggests that Fulvestrant is disrupting or changing Mad2, CENP-A or the nature of their interactions. We will need to further explore Fulvestrant to make conclusions about its mechanism of action in the cells and understand why a "growth rate rescue" in the MAD2-del/CENP-A-overexpression cells did not occur with this drug.

In the future, instead of selecting drugs where differential growth rates were seen across strains, the Mad2 "growth rate rescue" effect in the CENP-A-overexpressed cells should be further explored. Sodium Arsenate or Dasatinib could be further examined, since these drugs had a more dramatic growth rate increase from Mad2-normal/CENP-A-overexpression to Mad2-del/CENP-A-overexpression. Additionally, a growth assay on a control strain without the *PCK1_CSE4* insert should be performed. This would ensure that the insert did not affect the growth rate in any way, since all strains tested contained the inserted element. Overall, our results and proposed phenotypic "growth rate rescue" supports the idea that MAD2 dysregulation in cancer is a complex phenomenon that requires further study.

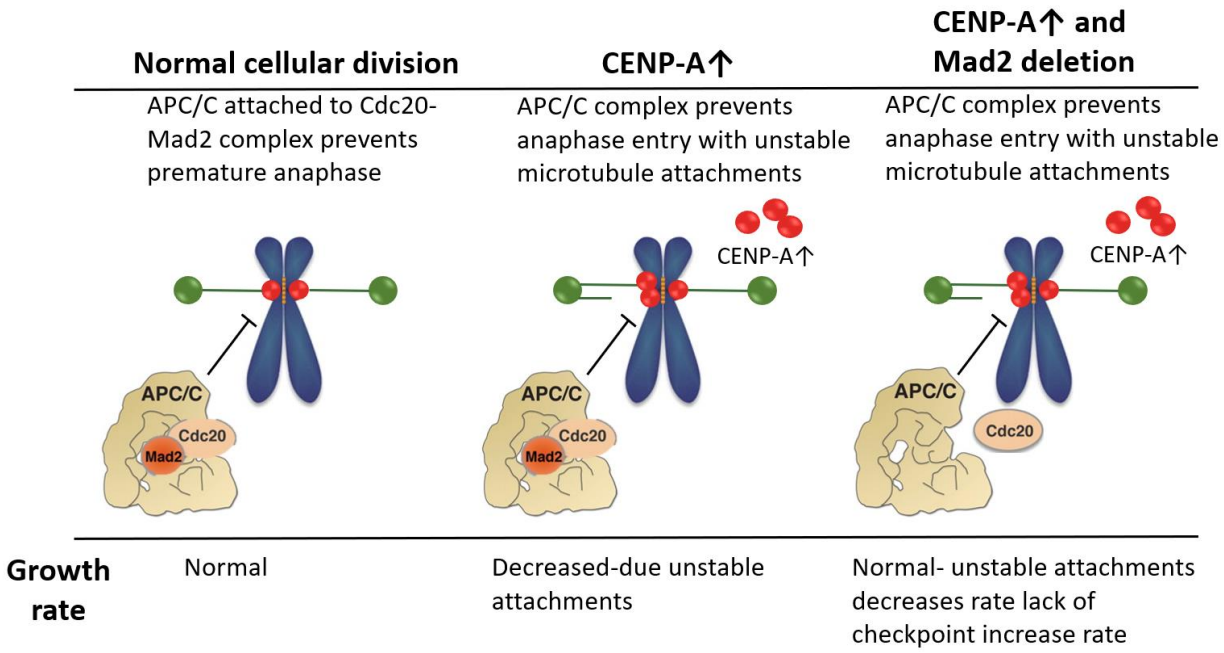

Figure 18: The proposed mechanism seen in *C. albicans* strains when CENP-A and Mad2 are altered. The deletion of Mad2 may recover the decreased growth rate of the CENP-A overexpressed cells. Since Mad2 is a checkpoint protein, lack of Mad2 will promote premature entry into anaphase, thus increasing the growth rate of cells compared to the cells with only CENP-A overexpression.

Chromosome loss rates do not reflect growth rate changes

To support the mechanism proposed in Figure 18 and explain growth rate changes, we examined chromosome loss rates in the Mad2-del strains with Fulvestrant and BPA. For the 5-FOA assay, no significant changes in mutation rates were seen. During the assay, high levels of variability were seen in the colony counts within each group. Although eight replicates are generally enough to obtain consistent results in a 5-FOA assay, the inconsistency in our data may suggest that for the strains we are using, we need to increase the sample size to obtain more accurate results. Chromosome loss assays are dependent on the loss of the selectable marker (in our case *URA3*). The *URA3* loss rate can vary based on chromosomal number and location. Both strains tested had the *URA3* on chromosome 5 in the same location and low loss rates were seen in both cases. Thus, we should test a control with *URA3* at a

different chromosomal location to determine if low loss rates were an artifact of the *URA3* location. If this is the case, any differences in loss rates between strains would be difficult to decipher.

Levels of CENP-A bound to the DNA is one determinant of kinetochore size (Sullivan et al., 2011). When CENP-A is overexpressed in *C. albicans*, increased levels are seen bound to the DNA (Burrack et al., 2011), suggesting that kinetochore size is also increased. A recent paper found that while cells with larger kinetochores are more error prone during mitosis, larger kinetochores also bi-orient (attach to microtubules) and line up in the middle of the cell more easily (Drpic et al., 2018). The balance between chromosome missegregation and increased mitotic efficiency seen with increased kinetochore size may cancel each other out. This would explain the lack of difference between loss rates in strains with normal and overexpressed CENP-A.

Although 5-FOA assays were not performed on Mad2-normal strains for technical reasons, we can compare our results to previously published chromosome loss data (Burrack et al., 2013). Strains with normal expression of CENP-A had a loss rate of 1.5×10^{-5} and strains with overexpressed CENP-A had a loss rate of 2×10^{-5}. In our Mad2-del strains (no drug), the mutation rate was 1.1×10^{-5} for normal CENP-A expression and 8×10^{-6} for the CENP-A-overexpressed cells. Since these chromosome loss rates are comparable to the published data without Mad2 deletion, one could speculate that the Mad2 deletion did not have a huge effect on the loss rates of cells. In the future, the technical issues with the Mad2-normal strain will be resolved and the loss rates compared across all four strains.

The lack of statistical significance in the loss rates and the comparable published loss rates suggest that the growth rate differences are not due to chromosomal loss. Growth rate differences could also be caused by cell cycle alterations. In the future, we hope to explore this possibility using DAPI (4',6-

diamidino-2-phenylindole) staining of cells and using fluorescence microscopy to compare the number of cells in each phase. This would provide information on cell cycle arrest.

If the growth differences can be explained by the cell cycle, this may suggest that kinetochore protein expression is globally altered by cell cycle changes. In this case, the drugs would affect the cell cycle, which would affect gene transcription levels that would result in differential growth rates. This supports the alternative hypothesis (Thiru et al., 2014), which states that coordinate upregulation of genes is a result of the cancer phenotype rather than a driver for it. In other words, the individual dysregulation of *MAD2* and *CSE4*/CENP-A would not drive cancer, but the drugs affecting the cell cycle may lead to dysregulation of the group of genes.

A-T.C-G

it's no wonder we love to read and
collect books and
write letters and
read poetry because

our souls are written in letters
paired twists fitting perfectly
together
A&T. C&G.

we are books held together by
sugar backbones and stardust
with transcripts revised and rewritten
for billions of years
your story is beauty and you are art

Conclusion

In cancer, Mad2 and CENP-A are often seen dysregulated but it is unclear whether their dysregulation drives the cancer or is a result of it. Here, we developed a system to study Mad2 and CENP-A dysregulation in *C. albicans* through differential gene expression and by determining compounds that inhibit the Mad2, CENP-A and interacting proteins. Growth assays of strains and compounds were performed to determine the growth rates in each condition. Mathematical modeling techniques were explored to analyze growth curves by fitting our data to logistic growth curves in R. A non-linear least squares technique was used to produce parameters for the population's carrying capacity, growth rate and lag period for each growth assay. In the assays, the growth rate of the double mutant (Mad2-

del/CENP-A-overexpression) was increased compared to the single mutant (Mad2-normal/CENP-A-overexpression) with normal Mad2 levels. We propose a mechanism that explains this “growth rate recovery” seen with Mad2 deletion when CENP-A is overexpressed. To test the mechanism, chromosome loss assays were performed in Fulvestrant and BPA but significant differences were not seen. We hypothesize that growth rate changes may be due to changes in the cell cycle and plan to explore this along with our proposed mechanism in the future using DAPI staining to obtain cell cycle data.

References

Alexandrov LB, Nik-Zainal S, Wedge DC, Aparicio SAJR, Behjati S, Biankin AV, Bignell GR, Bolli N, Borg A, Borresen-Dale AL, Boyault S, Burkhardt B, Butler AP, Caldas C, Davies HR, Desmedt C, Eils R, Eyfjord JE, Foekens JA, … Stratton, M. R. (2013). Signatures of mutational processes in human cancer. Nature 500, 415–421.

Alizadeh AA, Eisen MB, Davis RE, Ma C, Lossos IS, Rosenwald A, Boldrick JC, Sabet H, Tran T, Yu X, Powell JI, Yang L, Marti GE, Moore T, Hudson J, Lu L, Lewis DB, Tibshirani R, Sherlock G, Chan WC, Greiner TC, Weisenburger DD, Armitage JO, Warnke R, Levy R, Wilson W, Grever MR, Byrd JC, Botstein D, Brown PO, Staudt LM (2000). Distinct types of diffuse large B-cell lymphoma identified by gene expression profiling. Nature 403, 503–511.

Amato A, Schillaci T, Lentini L, Leonardo AD (2009). CENP-A overexpression promotes genome instability in pRb-depleted human cells. Molecular Cancer 8, 119-133.

Aneesh TP, Sekhar SM, Jose A, Chandran L, Zachariah SM (2009). Pharmacogenomics: The Right Drug to the Right Person. Journal of Clinical Medicine Research 1, 191–194.

Athwal RK, Walkiewicz, MP, Baek S, Fu S, Bui M, Camps J, Ried T, Sung MH, Dalal Y (2015). CENP-A nucleosomes localize to transcription factor hotspots and subtelomeric sites in human cancer cells. Epigenetics and Chromatin 8, 2.

Burrack L, Applen S, Berman J (2011). The requirement for the Dam1 complex is dependent upon the number of kinetochore proteins and microtubules. Current Biology 21, 889-896.

Burrack LS, Applen Clancy SE, Chacon JM, Gardner MK, Berman J (2013). Monopolin recruits condensin to organize centromere DNA and repetitive DNA sequences. Molecular Biology of the Cell 24, 2807-2819.

Burrack LS, Applen SE, Berman J (2011). The requirement for the Dam1 complex is dependent upon the number of kinetochore proteins and microtubules. Current Biology 21(10), 889–896.

Burrack LS, Hutton HF, Matter KJ, Clancey SA, Liachko I, Plemmons AE, Saha A, Power EA, Turman B, Thevandavakkam MA, Ay F, Dunham MJ, Berman J (2016). Neocentromeres Provide Chromosome Segregation Accuracy and Centromere Clustering to Multiple Loci along a *Candida albicans* Chromosome. PLOS Genetics 12, e1006317.

Chen X, Cheung ST, So S, Fan ST, Barry C, Higgins J, Lai KM, Ji J, Dudoit S, Ng IOL, Van de Rijn M, Botstein D, Brown PO (2002). Gene expression patterns in human liver cancers. Mol Biol Cell 13, 1929–1939.

Chi YH, Ward JM, Cheng LI, Yasunaga J, Jeang KT (2009). Spindle assembly checkpoint and p53 deficiencies cooperate for tumorigenesis in mice. Int J Cancer 124, 1483–1489.

Choi CM, Seo KW, Jang SJ, Oh YM, Shim TS, Kim WS, Lee DS, Lee SD (2009). Chromosomal instability is a risk factor for poor prognosis of adenocarcinoma of the lung: Fluorescence in situ hybridization analysis of paraffin-embedded tissue from Korean patients. Lung Cancer 64, 66–70.

Cortes-Ciriano I, van Westen GJ, Bouvier G, Nilges M, Overington JP, Bender A, Malliavin TE (2016). Improved large-scale prediction of growth inhibition patterns using the NCI60 cancer cell line panel. Bioinformatics 32, 85-95.

Davis AP, Grondin CJ, Johnson RJ, Sciaky D, King BL, McMorran R, Wiegers J, Wiegers TC, Mattingly CJ (2016). The Comparative Toxicogenomics Database: update 2017. Nucleic Acids Res 45, D972-978.

Davis AP, Grondin CJ, Johnson RJ, Sciaky D, King BL, McMorran R, Wiegers J, Wiegers TC, Mattingly CJ (2016). The Comparative Toxicogenomics Database: update 2017. Nucleic Acids Res 45, D972-D978.

DeLuca JG, Moree B, Hickey JM, Kilmartin JV, Salmon ED (2002). hNuf2 inhibition blocks stable kinetochore-microtubule attachment and induces mitotic cell death in HeLa cells. J Cell Biology 159, 549-55.

Diaz-Rodriguez E, Sotillo R, Schvartzman JM, Benerzra R (2008). Hec1 overexpression hyperactivates the mitotic checkpoint and induces tumor formation in vivo. Proc Natl Acad Sci USA 105, 16719-16724.

Drpic D, Almeida A, Aguiar P, Maiato H (2018). Chromosome (mis)segregation is biased by kinetochore size. bioRxiv doi:10.1101/278572.

Fallah Y, Brundage J, Allegakoen P, Shajahan-Haq AN (2017). MYC-Driven Pathways in Breast Cancer Subtypes. Biomolecules 7, 53.

Garber ME, Troyanskaya OG, Schluens K, Petersen S, Thaesler Z, Pacyna-Gengelbach M, van de Rijn M, Rosen GD, Perou CM, Whyte RI, Altman RB, Brown PO, Botstein D, Petersen I (2001). Diversity of gene expression in adenocarcinoma of the lung. Proceedings of the National Academy of Sciences of the United States of America 98, 13784–13789.

Ghayad SE, Bieche I, Vendrell JA, Keime C, Lidereau R, Dumontet C, Cohen PA (2008). mTOR inhibition reverses acquired endocrine therapy resistance of breast cancer cells at the cell proliferation and gene-expression levels. Cancer Sci 99, 1992-2003.

Hanahan D, Weinberg RA (2011). Hallmarks of Cancer: The Next Generation. Cell 144, 646-674.

Harrison BD, Hashemi J, Bibi M, Pulver R, Bavli D, Nahmias Y, Wellington M, Sapiro G, Berman J (2014). A Tetraploid Intermediate Precedes Aneuploid Formation in Yeasts Exposed to Fluconazole. PLoS Biol, e1001815.

Heilig CE, Loffler H, Mahlknecht U, Janssen JW, Ho AD, Jauch A, Kramer A (2010). Chromosomal instability correlates with poor outcome in patients with myelodysplastic syndromes irrespectively of the cytogenetic risk group. J Cell Mol Med 14, 895–902.

Hernando E, Nahle Z, Juan G, Diaz-Rodriguez E, Alaminos M, Hemann M, Michel L, Mittal V, Gerald W, Benezra R, Lowe SW (2004). Rb inactivation promotes genomic instability by uncoupling cell cycle progression from mitotic control. Nature 430, 797–802.

Hisaoka M, Matsuyama A, Hashimoto H (2008). Aberrant MAD2 expression in soft-tissue sarcoma. Pathology International 58, 329–333.

Holland AJ, Cleveland DW (2012). Losing balance: the origin and impact of aneuploidy in cancer. EMBO Rep 13, 501–514.

Kurosawa T, Hiroi H, Tsutsumi O, Ishikawa T, Osuga Y, Fujiwara T, Inoue S, Muramatsu M, Momoeda M, Taketani Y (2002). The Activity of Bisphenol A Depends on Both the Estrogen Receptor Subtype and the Cell Type. Endocrine Journal 49, 465-471.

Lagarde P, Pérot G, Kauffmann A, Brulard C, Dapremont V, Hostein I, Neuville A, Wozniak A, Sciot R, Schöffski P, Aurias A, Coindre JM, Debiec-Rychter M, Chibon F. 2012. Mitotic checkpoints and chromosome instability are strong predictors of clinical outcome in gastrointestinal stromal tumors. Clinical Cancer Research 18, 826-38.

Land H, Parada LF, Weinberg RA (1983). Tumorigenic conversion of primary embryo fibroblasts requires at least two cooperating oncogenes. Nature 304, 596–602.

Lawrence MS, Stojanov P, Polak P, Kryukov GV, Cibulskis K, Sivachenko A, Carter SL, Stewart C, Mermel CH, Roberts SA, Kiezun A, Hammerman PS, McKenna A, Drier Y, Zou L, Ramos AH, Pugh TJ, Stransky N, Helman E, Kim J, Sougnez C, Ambrogio L, Nickerson E, Shefler E, Cortés ML, Auclair D, Saksena G, Voet D, Noble M, DiCara D, Lin P, Lichtenstein L, Heiman DI, Fennell F, Imielinski M, Hernandez B, Hodis E, Baca S, Dulak AM, Lohr J, Landau DA, Wu CJ, Melendez-Zajgla J, Hidalgo-Miranda A, Koren A, McCarroll SA, Mora J, Crompton B, Onofrio R, Parkin M, Winckler W, Ardlie K, Gabriel SB, Roberts CWM, Biegel JA, Stegmaier K, Bass AJ, Garraway LA, Meyerson M, Golub TR, Gordenin DA, Sunyaev S, Lander ES, Getz G (2013). Mutational heterogeneity in cancer and the search for new cancer genes. Nature 499, 214–218.

Lea D, Coulson C (1949). The distribution of the numbers of mutants in bacterial populations. J Genetics 49, 264–285.

Li GQ, Li H, Zhang HF (2003). MAD2 and p53 expression profiles in colorectal cancer and its clinical significance. World J Gastroenterol 9, 1972-1975.

Li Y, Benezra R (1996). Identification of a human mitotic checkpoint gene: hsMAD2. Science 274, 246–248.

Lin CHA, Rhodes CT, Lin C, Phillips JJ, Berger MS (2017). Comparative analyses identify molecular signature of MRI-classified SVZ-associated glioblastoma. Cell Cycle 16, 765–775.

McClelland SE, Burrell RA, Swanton C (2009). Chromosomal instability: a composite phenotype that influences sensitivity to chemotherapy. Cell Cycle 8, 3262–3266.

Michel LS, Liberal V, Chatterjee A, Kirchwegger R, Pasche B, Gerald W, Dobles M, Sorger PK, Murty VVVS, Benezra R (2001). MAD2 haplo-insuficiency causes premature anaphase and chromosome instability in mammalian cells. Nature 409, 355–359.

Moriyama K, Tagami T, Akamizu T, Usui T, Saijo M, Kanamoto N, Hataya Y, Shimatsu A, Kuzuya H, Nakao K (2002). Thyroid Hormone Action Is Disrupted by Bisphenol A as an Antagonist. The Journal of Clinical Endocrinology & Metabolism 87, 5185–5190

Morschhauser J (2002). The genetic basis of fluconazole resistance development in *Candida albicans*. Biochim Biophys Acta 1587, 240–248.

Nathan MR, Schmid P (2017). A Review of Fulvestrant in Breast Cancer. Oncology and Therapy. 5, 17-29.

Negrini S, Gorgoulis VG, Halazonetis TD (2010). Genomic instability—an evolving hallmark of cancer. Nat Rev Mol Cell Biol 11, 220-228.

Nezi L, Rancati G, De Antoni A, Pasqualato S, Piatti S, Musacchio A (2006). Accumulation of MAD2–Cdc20 complex during spindle checkpoint activation requires binding of open and closed conformers of MAD2 in Saccharomyces cerevisiae . The Journal of Cell Biology 174, 39–51.

Nissen KK, Vogel U, Nexo BA (2009). Association of a single nucleotide polymorphic variation in the human chromosome 19q13.3 with drug responses in the NCI60 cell lines. Anticancer Drugs 20, 174–178.

Percy MJ, Myrie KA, Neeley CK, Azim JN, Ethier SP, Petty EM (2000). Expression and mutational analyses of the human MAD2L1 gene in breast cancer cells. Genes Chromosomes Cancer 29, 356–362.

Pinto M, Soares MJ, Cerverira N, Henrique R, Ribeiro FR, Oliveria J, Jeronimo C, Teixeira MR (2007). Expression changes of the MAD mitotic checkpoint gene family in renal cell carcinomas characterized by numerical chromosome changes. Virchows Arch 450, 379–385.

R2: Genomics Analysis and Visualization Platform (http://r2.amc.nl).

Rimkus C, Friederichs J, Rosenberg R, Holzmann B, Siewert JR, Janssen KP (2007). Expression of the mitotic checkpoint gene MAD2L2 has prognostic significance in colon cancer. Int. J. Cancer 120, 207–211.

Savas S, Azorsa DO, Jarjanazi H, Ibrahim-Zada I, Gonzales IM, Arora S, Henderson MC, Choi YH, Briollais L, Ozcelik H, Tuzmen S. NCI60 cancer cell line panel data and RNAi analysis help identify EAF2 as a modulator of simvastatin and lovastatin response in HCT-116 cells. PLoS One 20114, e18306.

Scafoglio C, Ambrosino C, Cicatiello L, Altucci L, Ardovino M, Bontempo P, Medici N, Molinari AM, Nebbioso A, Facchiano A, Calogero RA, Elkon R, Menini N, Ronzone R, Biglia N, Sismondi P, De Bortoli M, Weisz A (2006). Comparative gene expression profiling reveals partially overlapping but distinct genomic actions of different antiestrogens in human breast cancer cells. J Cell Biochem 98, 1163-84.

Scherf U, Ross DT, Waltham M, Smith LH, Lee JK, Lanabe L, Kohn KW, Reinhold WC, Myers TG, Andrews DT, Scudiero DA, Eisen MB, Sausville EA, Pommier Y, Botstein D, Brown PO, Weinstein JN (2000). Nature Genetics 24, 227-234.

Schvartzman JM, Sotillo R, Benezra R (2010). Mitotic chromosomal instability and cancer: mouse modelling of the human disease. Nature Reviews Cancer 10(2), 102-105.

Schvartzman JM, Sotillo R, Benezra R (2010). Mitotic chromosomal instability and cancer: mouse modelling of the human disease. Nature Rev. Cancer 10, 102–115.

Sheltzer JM (2013). A transcriptional and metabolic signature of primary aneuploidy is present in chromosomally-unstable cancer cells and informs clinical prognosis. Cancer Research 73, 6401–6412.

Shrestha RL, Ahn GS, Staples MI, Sathyan KM, Karpova TS, Foltz DR, Basrai MA (2017). Mislocalization of centromeric histone H3 variant CENP-A contributes to chromosomal instability (CIN) in human cells. Oncotarget 8 (29), 46781-46800.

Sotillo R, Schvartzman JM, Socci ND, Benezra R (2010). MAD2-induced chromosome instability leads to lung tumor relapse after oncogene withdrawal. Nature 464(7287), 436–440.

Sotillo R, Schvartzman JM, Socci ND, Benezra R (2010). MAD2-induced chromosome instability leads to lung tumor relapse after oncogene withdrawal. Nature 464, 436-440.

Spell RM, Jinks-Robertson S (2004). Determination of mitotic recombination rates by fluctuation analysis in Saccharomyces cerevisiae. Methods Mol Biol 262, 3–12.

Sullivan LL, Boivin CD, Mravinac B, Song IY, Sullivan BA (2011). Genomic size of CENP-A domain is proportional to total alpha satellite array size at human centromeres and expands in cancer cells. Chromosome Research: An International Journal on the Molecular, Supramolecular and Evolutionary Aspects of Chromosome Biology 19, 457–470.

Sun X, Clermont PL, Jiao W, Helgason CD, Gout PW, Wang Y, Qu S (2016). Elevated expression of the centromere protein-A(CENP-A)-encoding gene as a prognostic and predictive biomarker in human cancers. Int J Cancer 139, 899-907.

Sushama S, Gorbsky GJ (2015). Spatiotemporal regulation of the anaphase promoting complex in mitosis. Nature Reviews Molecular Cell Biology 16, 82-94.

Swanton C, Nicke B, Schuett M, Eklund AC, Ng C, Li Q, Hardcastle T, Lee A, Rov R, East P, Kschischo M, Endesfelder D, Wylie P, Kim SN, Chen JG, Howell M, Ried T, Habermann JK, Auer G, Brenton JD, Szallasi Z, Downward J (2009). Chromosomal instability determines taxane response. Proc Natl Acad Sci USA 106, 8671–8676.

Sze KM, Ching YP, Jin DY, Ng IO (2004). Association of MAD2 expression with mitotic checkpoint competence in hepatoma cells. J Biomed Sci 11, 920–927.

Szklarczyk D, Morris JH, Cook H, Kuhn M, Wyder S, Simonovic M, Santos A, Doncheva NT, Roth A, Bork P, Jensen LJ, von Mering C (2017). The STRING database in 2017: quality-controlled protein-protein association networks, made broadly accessible. Nucleic Acids Res 45, D362-368.

Szklarczyk D, Morris JH, Cook H, Kuhn M, Wyder S, Simonovic M, Santos A, Doncheva NT, Roth A, Bork P, Jensen LJ, von Mering C (2017). The STRING database in 2017: quality-controlled protein-protein association networks, made broadly accessible. Nucleic Acids Res 45, D362-68.

Tanaka K, Nishioka J, Kato K, Nakamura A, Mouri T, Miki C, Kusunoki M, Nobori T (2001). Mitotic Checkpoint Protein hsMAD2 as a Marker Predicting Liver Metastasis of Human Gastric Cancers. Japanese Journal of Cancer Research 92, 952–958.

Thiru P, Kern DM, McKinley KL, Monda JK, Rago F, Su KC, Tsinman T, Yarar D, Bell GW, Cheeseman IM (2014). Kinetochore genes are coordinately up-regulated in human tumors as part of a FoxM1-related cell division program. Microbiology of the Cell 25, 1983-1994.

Tomonaga T, Matsushita K, Yamaguchi S, Oohashi T, Shimada H, Ochiai T, Yoda K, Nomura F (2003). Overexpression and mistargeting of centromere protein-A in human primary colorectal cancer. Cancer Res 63, 3511–3516.

Vader G, Lens SM (2008). The Aurora kinase family in cell division and cancer. Biochem Biophys Acta 1786, 60–72.

van 't Veer LJ, Dai H, van de Vijver MJ, He YD, Hart AA, Mao M, Peterse HL, van der Kooy K, Marton MJ, Witteveen AT, Schreiber GJ, Kerkhoven RM, Roberts C, Linsley PS, Bernards R, Friend SH (2002). Gene expression profiling predicts clinical outcome of breast cancer. Nature 415, 530–536.

Vandenberg LN, Maffini MV, Sonnenschein C, Rubin BS, Soto AM (2009). Bisphenol-A and the great divide: a review of controversies in the field of endocrine disruption. Endocr Rev 30, 75-95.

Verdaasdonk JS, Bloom K (2011). Centromeres: unique chromatin structures that drive chromosome segregation. Nature Reviews. Molecular Cell Biology 12, 320–332.

Villarroel MC, Rajeshkumar NV, Garrido-Laguna I, De Jesus-Acosta A, Jones S, Maitra A, Hruban RH, Eshleman JR, Klein A, Laheru D, Donehower R, Hidalgo M (2011). Personalizing cancer treatment in the age of global genomic analyses: PALB2 gene mutations and the response to DNA damaging agents in pancreatic cancer. Mol Cancer Ther 10,3–8.

Vogelstein B, Papadopoulos N, Velculescu VE, Zhou S, Diaz LA, Kinzler KW (2013). Cancer Genome Landscapes. Science 339, 1546–1558.

Wadia PR, Cabaton NJ, Borrero MD, Rubin BS, Sonnenschein C, Shioda T, Soto AM (2013). Low-dose BPA exposure alters the mesenchymal and epithelial transcriptomes of the mouse fetal mammary gland. PLoS One 8, e63902.

Wakeling AE, Bowler J (1987). Steroidal pure antioestrogens. J Endocrinol 112, R7-10.

Wang L, Yin F, Du Y, Du W, Chen B, Zhang Y, Wu K, Ding J, Liu J, Fan D (2009). MAD2 as a Key Component of Mitotic Checkpoint: A Probable Prognostic Factor for Gastric Cancer, American Journal of Clinical Pathology 131, 793–801.

Wang X, Jin DY, Ng RW, Feng H, Wong YC, Cheung AL, Tsao SW (2002). Significance of MAD2 expression to mitotic checkpoint control in ovarian cancer cells. Cancer Res 62, 1662–1668.

Wang X, Jin DY, Wong YC, Cheung AL, Chun AC, Lo AK, Liu Y, Tsao SW (2000). Correlation of defective mitotic checkpoint with aberrantly reduced expression of MAD2 protein in nasopharyngeal carcinoma cells. Carcinogenesis 21, 2293–2297.

Wardley AM (2002). Fulvestrant: a review of its development, pre-clinical and clinical data. Int J Clin Pract 56, 305-309.

Weaver BA, Cleveland DW (2006). Does aneuploidy cause cancer? Curr Opin Cell Biol 18, 658–667.

Wu Q, Qian YM, Zhao XL, Wang SM, Feng XJ, Chen XF, Zhang SH (2012). Expression and prognostic significance of centromere protein A in human lung adenocarcinoma. Lung Cancer 77, 407-414.

Yoon DS, Wersto RP, Zhou W, Chrest FJ, Garrett ES, Kwon TK, Gabrielson E (2002). Variable levels of chromosomal instability and mitotic spindle checkpoint defects in breast cancer. Am J Pathol 161, 391–397.

Zhang W, Mao JH, Zhu W, Jain AK, Liu K, Brown JB, Karpen GH (2016). Centromere and kinetochore gene misexpression predicts cancer patient survival and response to radiotherapy and chemotherapy. Nature Communications 7, 12619.